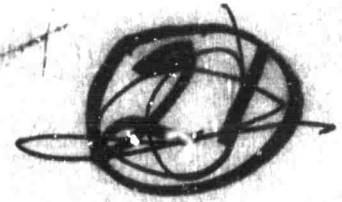
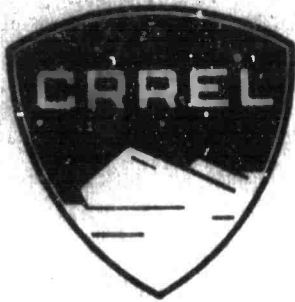


TR 225



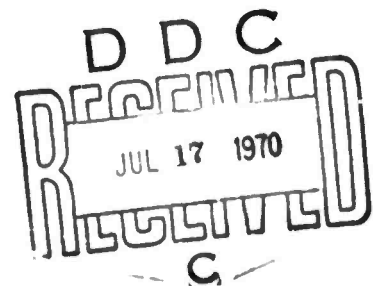
Technical Report 225

298802AD

THE ISOTHERMAL COMPRESSIBILITY OF FROZEN SOIL AND ICE TO 30 KILOBARS AT -10°C

Edwin Chamberlain
and
Pieter Hoekstra

June 1970



CONDUCTED FOR
ADVANCED RESEARCH PROJECTS AGENCY
BY

CORPS OF ENGINEERS, U.S. ARMY
COLD REGIONS RESEARCH AND ENGINEERING LABORATORY
HANOVER, NEW HAMPSHIRE

THIS DOCUMENT HAS BEEN APPROVED FOR PUBLIC RELEASE
AND SALE: ITS DISTRIBUTION IS UNLIMITED.

43

**BEST
AVAILABLE COPY**

THE ISOTHERMAL COMPRESSIBILITY OF FROZEN SOIL AND ICE TO 30 KILOBARS AT -10°C

**Edwin Chamberlain
and
Pieter Hoekstra**

June 1970

**CONDUCTED FOR
ADVANCED RESEARCH PROJECTS AGENCY
BY**

**CORPS OF ENGINEERS, U.S. ARMY
COLD REGIONS RESEARCH AND ENGINEERING LABORATORY
HANOVER, NEW HAMPSHIRE**

**THIS DOCUMENT HAS BEEN APPROVED FOR PUBLIC RELEASE
AND SALE; ITS DISTRIBUTION IS UNLIMITED.**

PREFACE

This study was conducted by Mr. Edwin Chamberlain, Research Civil Engineer, Applied Research Branch (Mr. Albert F. Wuori, Chief), Experimental Engineering Division (Mr. Kenneth A. Linell, Chief), and Dr. Pieter Hoekstra, Research Physicist, Earth Sciences Branch (Dr. Duwayne M. Anderson, Chief), Research Division (Dr. Kay F. Sterrett, Chief), U.S. Army Cold Regions Research and Engineering Laboratory.

The research was supported by the Advanced Research Projects Agency of the Department of Defense under ARPA Order 968.

The authors express their gratitude to Mr. Roscoe Perham for his assistance and cooperation in the research program. They specially thank Dr. Douglas Stephens of the Lawrence Radiation Laboratory for his advice and assistance. Specialist 5 Robert Keune prepared the samples and processed the data. His help in completing this work on time was very valuable.

The report was technically reviewed by Mr. L. David Minsk and Mr. Richard McGaw.

The contents of this report are not to be used for advertising, publication, or promotional purposes. Citation of trade names does not constitute an official endorsement or approval of the use of such commercial products.

CONTENTS

	Page
Preface	ii
Symbols	v
Introduction	1
Apparatus	3
Sample description	5
Ottawa banding sand	5
West Lebanon glacial till	5
Ice	5
Specimen preparation	7
Testing procedure and data evaluation	7
The compressibility of ice at -10C	10
The compressibility of frozen sand and silt at -10C	15
The compressibility of fully saturated frozen ground	20
The compressibility of partially frozen ground	21
Conclusions	25
Literature cited	25
Appendix A. Isothermal compressibility data	27
Abstract	35

ILLUSTRATIONS

Figure

1. Encapsulated sample and high pressure die	2
2. Test apparatus in loading machine	2
3. Isothermal compressibility test apparatus	3
4. Example of raw data for saturated frozen soil (2nd compression curve)	4
5. Example of raw data for gold (3rd compression curve) ..	4
6. Gradations of the soils tested	5
7. Set correction for gold	8
8. Specimen configuration before and after loading	8
9. Phase diagram of water in the temperature-pressure plane	11
10. Predicted isothermal compressibility of ice at -10C and water at + 5C	14
11. Isothermal compressibility of ice, specimen 11	14
12. Isothermal compressibility of ice, specimen 43	14
13. Isothermal compressibility of ice, specimen 44	14
14. Isothermal compressibility of fully saturated Ottawa banding sand, specimen 1	15
15. Isothermal compressibility of fully saturated Ottawa banding sand, specimen 18	15
16. Isothermal compressibility of fully saturated Ottawa banding sand, specimen 24	15

ILLUSTRATIONS (Cont'd)

Figure	Page
17. Isothermal compressibility of fully saturated Ottawa banding sand, specimen 27	15
18. Isothermal compressibility of fully saturated West Lebanon glacial till, specimen 32	16
19. Isothermal compressibility of fully saturated West Lebanon glacial till, specimen 42	16
20. Isothermal compressibility of partially saturated Ottawa banding sand, specimen 34	16
21. Isothermal compressibility of partially saturated Ottawa banding sand, specimen 17	16
22. Isothermal compressibility of partially saturated Ottawa banding sand, specimen 28	17
23. Isothermal compressibility of partially saturated Ottawa banding sand, specimen 33	17
24. Isothermal compressibility of partially saturated Ottawa banding sand, specimen 29	18
25. Isothermal compressibility of dry Ottawa banding sand, specimen 31	18
26. Isothermal compressibility of dry Ottawa banding sand, specimen 35	19
27. Isothermal compressibility of partially saturated West Lebanon glacial till, specimen 16	19
28. Isothermal compressibility of partially saturated West Lebanon glacial till, specimen 40	19
29. First and second compressibilities of fully saturated Ottawa banding sand, specimen 24	24
30. First, second and third compressibilities of dry Ottawa banding sand, specimen 35	24
31. The isothermal compressibility of indium	24

TABLES

Table	
I. Material index properties	6
II. Summary of sample index properties	6
III. Specific volume of water and ice I on the equilibrium curve	11
IV. Specific volume of water and ice V on the equilibrium curve	11
V. Specific volume change on the ice V-ice VI equilibrium curve	12
VI. Specific volume change on the ice VI-ice VII equilibrium curve	12
VII. Compressibility of ice	13

SYMBOLS

a, b	Compressibility coefficients
$B_a, B_b, B_c, \text{ etc.}$	Volume compressibilities of each mineral component
B_r	Reuss average
B_v	Voigt average
D	Depth to upper seal for any test specimen
D_g	Depth to upper seal for gold
D_0	Die bore diameter at atmospheric pressure
D_s	Depth to upper seal for soil or ice specimens
D_t	Die bore diameter at any pressure
E	Young's modulus
F	Piston load
l	Specimen length
n	Porosity
P	True pressure
P_a	Apparent pressure
S	Residual piston displacement for any test specimen
S_c	Set correction
S_g	Residual piston displacement for gold
S_i	Degree of saturation with ice
S_s	Residual piston displacement for soil or ice specimens
v_i^0	Specific volume of ice at atmospheric pressure
v_i^P	Specific volume of ice at any pressure
V/V_0	Relative volume
$V_a, V_b, V_c, \text{ etc.}$	Volume percentages of each mineral component
V_a^0	Volume of air voids at atmospheric pressure
V_g^0	Volume of gold at atmospheric pressure
V_i^0	Volume of ice at atmospheric pressure
V_m^0	Volume of mineral solids at atmospheric pressure
V_s^0	Volume of test specimen at atmospheric pressure

SYMBOLS (Cont'd)

V_s^p	Volume of test specimen at any pressure
V_v^0	Volume of voids at atmospheric pressure
a	Ratio of minor to major radius of a rock cavity
ρ_d	Dry density
ρ	Total or wet density
Δ_{g+m}	Apparent axial deformation of gold specimen
Δ'_{g+m}	Adjusted axial deformation of gold specimen
Δ_{s+m}	Apparent axial deformation of soil or ice specimen
$\Delta V/V_0$	Change in relative volume
ΔV_0	Change in volume of air
ΔV_g	True change in volume of gold specimen
ΔV_{g+m}	Apparent change in volume of gold specimen
ΔV_i	Change in volume of ice component
ΔV_m	Change in volume of mineral component
ΔV_s	True change in volume of test specimen
ΔV_{s+m}	Apparent change in volume of test specimen

THE ISOTHERMAL COMPRESSIBILITY OF FROZEN SOIL AND ICE TO 30 KILOBARS AT -10C

by

Edwin Chamberlain and Pieter Hoekstra

INTRODUCTION

The objective of this program was to investigate the compressibility of frozen soils and ice in the pressure region of 0 to 30 kbars at -10C. The data were obtained for use in model calculations for mound and cavity growth and shock wave transmission during a nuclear or high-explosive cratering event in frozen ground. The wide variation of the properties of *in situ* frozen soils with location precludes the direct use of the reported test results for a particular site. Therefore, emphasis has been placed on isolating the physical properties of frozen soils that determine the compressibility so that the compressibility of *in situ* frozen soils can be predicted from convenient measurable parameters.

Frozen soils consist of a matrix of mineral grains with pore spaces that may be filled with ice (water) and air. The problem of prediction of compressibilities falls into two categories: those for saturated frozen ground and those for partially saturated frozen ground. For saturated frozen ground the compressibility can be predicted from the constituent components, ice and mineral. The required parameters are the volumetric proportions and the compressibilities of the mineral components and the ice. For partially saturated frozen ground, in addition to these parameters, the closure of the pore spaces due to the crushing of the grains must be evaluated. This problem remains partially unsolved. As will be demonstrated, this appears to be significant only for soil with a low degree of saturation.

Bridgman (1911, 1912, 1914, and 1937) was the first to investigate the compressibility of water and its many ice phases to high pressures. His work is the basis for this discussion. Other investigators (Whalley *et al.*, 1966; Brown and Whalley, 1966; Wilson, *et al.*, 1965) have studied the phase diagram of water in the pressure-temperature plane but have not made volume change observations.

Numerous investigators (Adams and Williamson, 1923; Bassett *et al.*, 1968; Bridgman, 1964; Brown *et al.*, 1967; Stephens, 1964; Stephens and Lilley, 1966; Walsh, 1965, a,b) have studied the compressibility of minerals, soils, and rocks to high pressures.

A piston-die device with which a uniaxial load is imposed on a lead-encapsulated specimen was used for these tests. The die restrains the encapsulated specimen from lateral expansion. Load and deformation measurements are continuously recorded. The compressibility of gold is used as a standard to provide a continuous calibration of the loading apparatus.

The techniques and operational procedures were developed with the aid of personnel of the Lawrence Radiation Laboratory, Livermore, California.

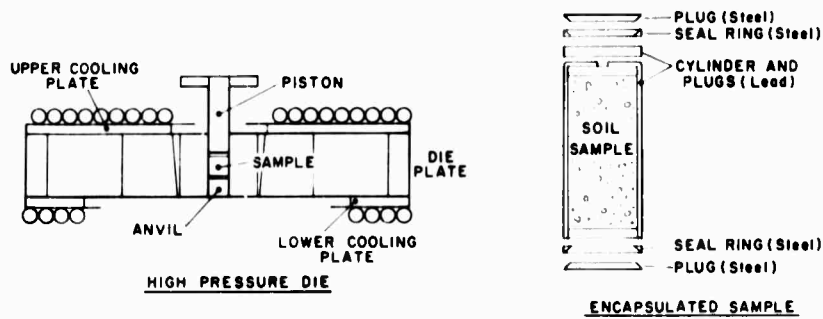


Figure 1. Encapsulated sample and high pressure die.

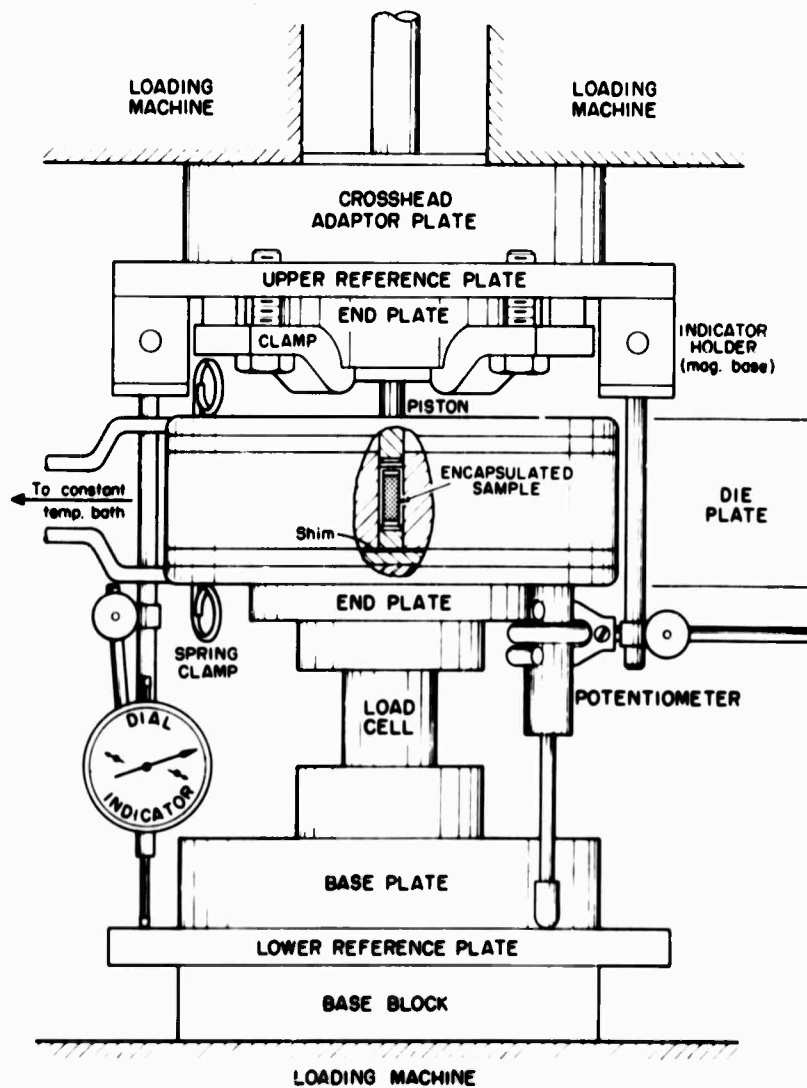


Figure 2. Test apparatus in loading machine.

APPARATUS

The experimental procedure and isothermal compression apparatus are similar to those described by Stephens (1964). The test samples were nominally 1.168 mm in diameter and 2.540 mm long. Each was encapsulated in lead and compressed between two 1.27-cm-diam carbide pistons while confined in the bore of a die plate (see Fig 1 and 2). Hardened steel rings and plugs prevented extrusion of the lead.

The piston was loaded by a Tinius-Olsen Universal, screw-type testing machine (see Fig. 3) at a rate slow enough to obviate any compressive heating effects (≈ 40 min/cycle). The tests were conducted in a coldroom maintained at approximately -10°C . To obtain a more precise temperature control, a coolant was circulated through coils attached to the die plate. The coolant was maintained at a temperature of $-10 \pm 0.5^{\circ}\text{C}$ by a constant temperature bath. The die temperature was sensed by a glass bead thermistor and recorded at intervals. The piston displacement was measured by a linear film potentiometer and the load by a load cell. The load and displacement were recorded on an X-Y plotter. Typical records are shown in Figures 4 and 5.

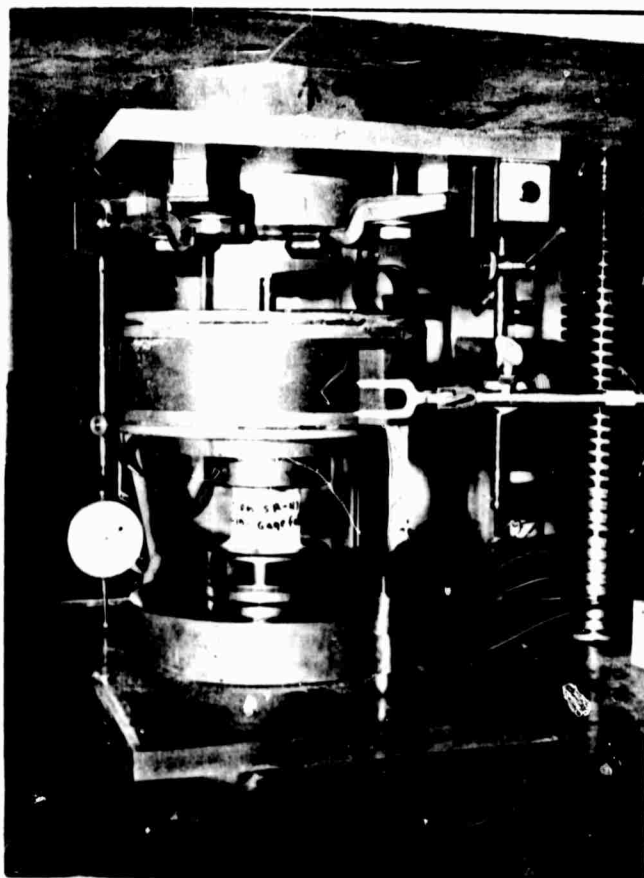


Figure 3. Isothermal compressibility test apparatus.

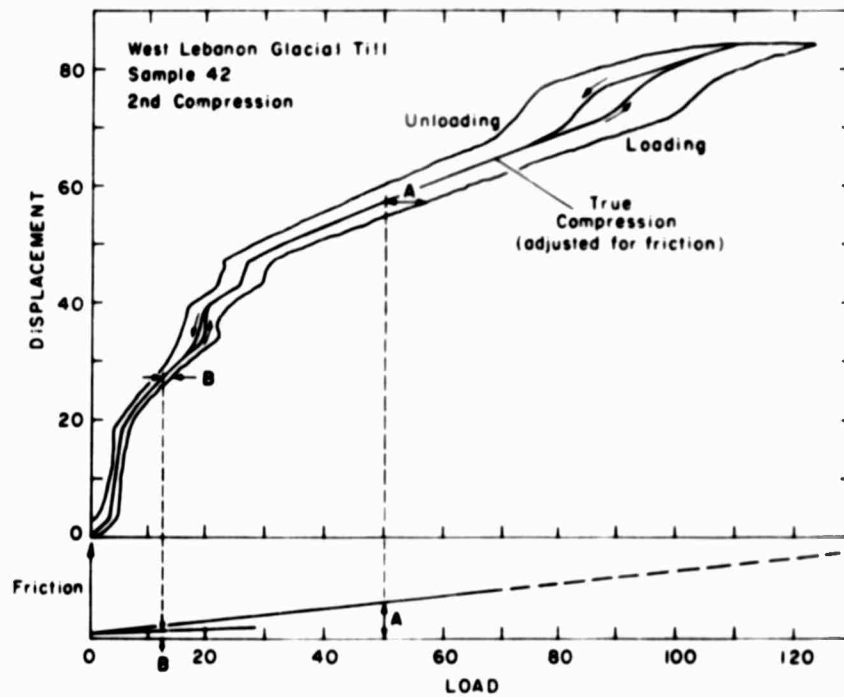


Figure 4. Example of X-Y plots for saturated frozen soil (2nd compression curve).

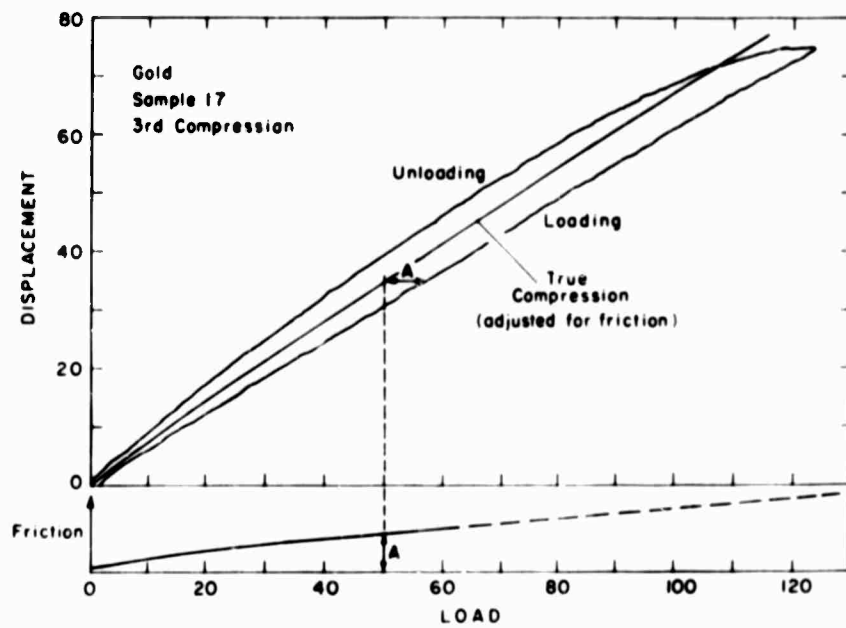


Figure 5. Example of X-Y plots for gold (3rd compression curve).

SAMPLE DESCRIPTION

The relevant index properties and gradations of the materials tested are shown in Table I and Figure 6. The test specimens included two soils: West Lebanon glacial till (WLGT) and Ottawa banding sand (OWS). They were prepared at various degrees of saturation (see Table II). In addition, tests were conducted on clear polycrystalline ice.

Ottawa banding sand

This material was well rounded, well sorted quartz sand with a median diameter of $100\ \mu$ and 100% of the material falling between 74 and $149\ \mu$. The material was selected for its high porosity and granular nature, to allow sands and gravels to be modeled. The nature of the test program restricted the maximum particle size to $149\ \mu$. The monomineralic structure of the sand permitted more meaningful comparison with previous results for pure quartz.

West Lebanon glacial till

This material was an extremely well graded till with particles having a maximum diameter of $149\ \mu$ and a mean diameter of $36\ \mu$. This gradation contained a high percentage of fine-grained materials in contrast to the gradation of Ottawa banding sand. This material was cut from a boundary till and in its test form was classified silt (ML) according to the Soil Classification System.

Ice

This material was a clear polycrystalline columnar ice having a maximum grain diameter of $0.5\ \text{cm}$, with the c-axis in the direction of compression.

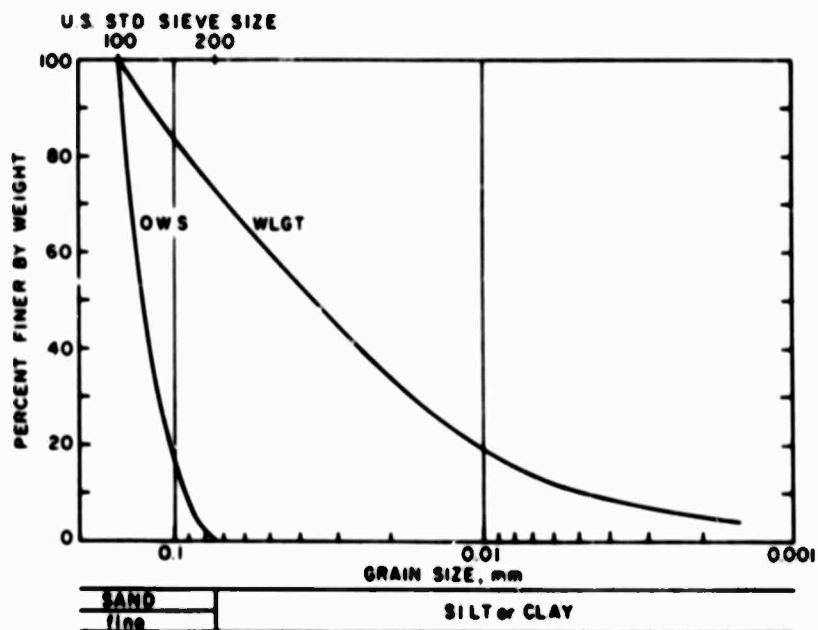


Figure 6. Gradations of the soils tested.

ISOTHERMAL COMPRESSIBILITY OF FROZEN SOIL AND ICE

Table I. Material index properties.

Unified Soil Classification	Apparent sp. gr. of solids	Liquid* limit	Plastic* limit	Plasticity* index	Max. dry density (g/cm ³)	Optimum water content (%)
Ottawa banking sand (OWS)						
Sand (SP)	2.65			non-plastic	1.91	
West Lebanon glacial till (WLGT)						
Silt (ML)	2.86	16.2	18.4	non-plastic	1.91	12.2
Polycrystalline ice						
	0.917					

* Atterberg limits.

Table II. Summary of sample index properties.

Sample	Porosity	Dry density (g/cm ³)	Wet density (g/cm ³)	Sat. with ice (%)
Polycrystalline ice				
11			0.917	
43			.917	
44			.917	
West Lebanon glacial till				
16	0.367	1.842	2.040	58.3
40	.364	1.852	2.030	57.3
32	.364	1.847	2.172	100.0
42	.366	1.838	2.172	100.0
Ottawa banking sand				
1	0.378	1.639	2.002	100.0
18	.454	1.438	1.850	100.0
24	.373	1.650	1.985	100.0
27	.373	1.651	1.990	100.0
34	.373	1.651	1.903	75.6
17	.427	1.507	1.940	55.7
26	.373	1.651	1.880	50.9
29	.373	1.651	1.732	25.2
33	.372	1.651	1.732	25.1
35	.372	1.651	1.651	0
31	.372	1.651	1.651	0

SPECIMEN PREPARATION

All soil specimens were prepared in 1.168-cm-ID lead capsules approximately 3.2 cm long, with a wall thickness of 0.051 cm. The specimen length was approximately 2.4 cm. This provided approximately 0.8 cm excess lead for sealing the capsule.

The West Lebanon glacial till specimens were compacted wet by tamping with a 1.15-cm-diam rod. The Ottawa banding sand specimens were compacted dry by vibration. The water content of each specimen was adjusted to the desired value after compaction. Saturated soil specimens were wetted under vacuum. All soil specimens were frozen rapidly in a -10°C coldroom and allowed to temper for at least 24 hours.

The ice specimens were frozen from de-aired distilled water in a 7.5-cm-diam plastic tube, machined to size, and placed in the lead capsules. The ice specimens were also tempered for 24 hours at -10°C.

TESTING PROCEDURE AND DATA EVALUATION

The primary data were generated by loading and unloading the test samples to and from a pressure of approximately 30 kbars. The load and the corresponding displacement signals were recorded continuously (Fig. 4, 5); the recordings resulted in a loop. This hysteresis was primarily the result of the internal friction in the test specimen, the friction between the lead and the wall of the die bore, and the irreversible closure of soil voids. The techniques used to correct for friction required a closed loop. Thus, each specimen was subjected to several compression cycles until a closed loop was obtained.

The friction was assumed to be equal upon loading and unloading; the average of the two traces represented the compressibility of the material. The friction increased with load. The friction-load relationship was assumed to be unique for each material and not influenced by heat of compression or by structural changes from one cycle to the next. For the partially saturated soil samples, the compressibility was obtained from the first compression curve inasmuch as the subsequent compressions resulted in the irreversible closure of the soil voids. The friction correction for the first compression cycle was obtained from the closed-loop compression curve. For the fully saturated specimens and polycrystalline ice, the friction-corrected closed-loop compression curve was used to compute the sample compressibility. It was assumed that there was no material loss during the loading and unloading cycles. In many cases, the lead capsule containing the soil specimen ruptured, resulting in a moisture loss. These tests were disregarded.

After friction corrections were applied, the loading-unloading curves for the fully saturated specimens and for the ice still exhibited some hysteresis (see Fig. 4). This hysteresis is probably related to the rate effects associated with the phase transition.

To correct for mechanical effects external to the sample a differential technique was used: the compressibility of the test specimen was compared with that of gold (Bridgman, 1940; Stephens and Lilley, 1967). Every second sample tested was gold.

To adjust the displacements of the gold samples and the displacements of the test sample to a common datum further correction was applied. Each test sample was preloaded to 50 lb. This load was selected because it was large enough to cause seating of the seals but not so large as to cause significant deformation of the test sample. The load was released, the piston was removed and the depth to the upper seal D (See Fig. 7) was measured with a depth micrometer. The piston

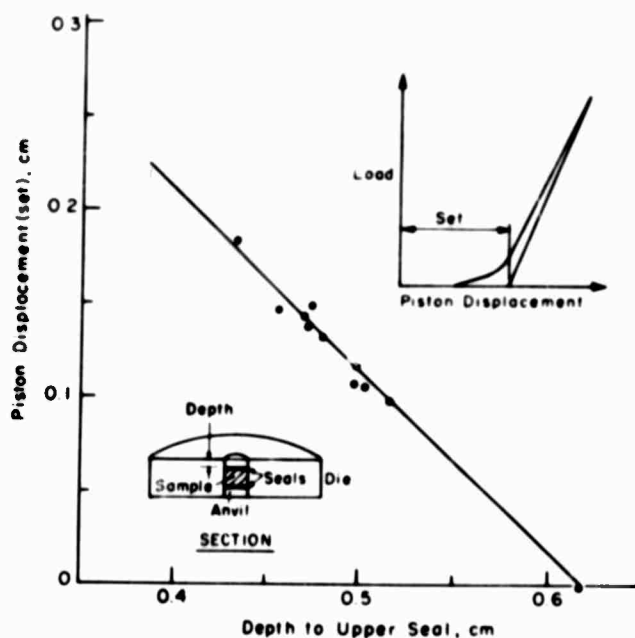


Figure 7. Set correction for gold.

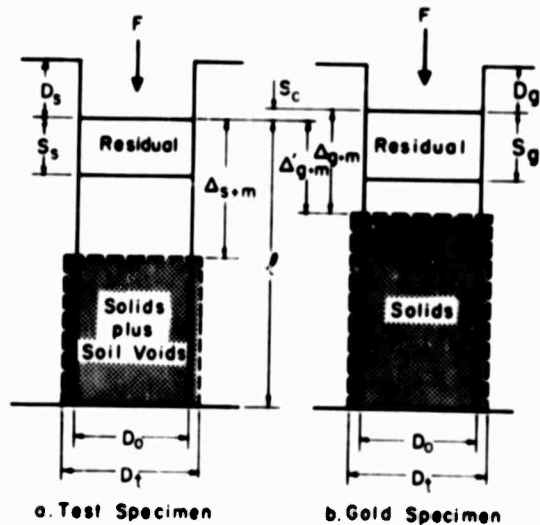


Figure 8. Specimen configuration before and after loading.

was replaced and the test continued. Dial gauge readings were observed at a 50-lb load before and after loading. For the gold samples, the difference between these readings represented the residual displacement required to fill all voids between the seals with lead (the lead would flow under pressure). This piston displacement is called the set S . It is plotted versus D for gold in Figure 7, resulting in the linear expression:

$$S = 0.596 - 0.965D. \quad (1)$$

The normalizing of the gold runs to the soil or ice runs is accomplished in the following manner. The set S corresponding to the D for the test sample is found from eq 1. The set correction S_c required to adjust the apparent axial deformation of the gold Δ_{g+m} to the same datum as the test specimen is equal to the difference between the calculated set for the test sample and the measured set for the gold (see Fig 8). The adjusted axial deformation of the gold Δ'_{g+m} at any load F is thus:

$$\Delta'_{g+m} = \Delta_{g+m} - S_c \quad (2)$$

The use of this relationship requires that the same total volume of material be contained between the seals for all runs.

Another correction was made to account for the expansion of the die bore under pressure. Stephens and Lilley (1967) gave a table relating the true pressure P to the apparent pressure P_a . Fitting a straight line to their data resulted in the following relationship:

$$P = 0.988 P_a \quad (3)$$

The true change in the volume of the test specimen ΔV_s is related to the apparent change in the volume of the test specimen ΔV_{s+m} , the apparent change in the volume of the gold specimen ΔV_{g+m} , and the true change in the volume of the gold specimen ΔV_g in the following expression:

$$\Delta V_s = \Delta V_{s+m} - \Delta V_{g+m} + \Delta V_g \quad (4)$$

The apparent change in the volume of the gold is equal to the average value for the gold runs before and after loading.

Figure 8 illustrates the specimen configurations before and after loading. The assumed deformation under load is cylindrical. The actual deformed shape is probably more barrel-like, but the difficulties in the evaluation of such a shape lead us to the cylindrical approximation. The apparent change in the volume of the test specimen ΔV_{s+m} is found as follows:

$$\begin{aligned} \Delta V_{s+m} &= \frac{\pi D_0^2}{4} l - (l - \Delta_{s+m}) \frac{\pi D_t^2}{4} \\ &= \frac{\pi}{4} (l D_0^2 - l D_t^2 + \Delta_{s+m} D_t^2). \end{aligned} \quad (5)$$

From eq 3 the die bore diameter at any pressure D_t can be related to the die bore diameter at atmospheric pressure D_0 by the following expression:

$$D_t^2 = \frac{D_0^2}{0.988} \quad (6)$$

Substituting eq 6 in eq 5 gives:

$$\Delta V_{s+m} = \frac{\pi D_0^2}{4} \left(l - \frac{l}{0.988} + \frac{\Delta_{s+m}}{0.988} \right) \quad (7)$$

Similarly:

$$\Delta V_{g+m} = \frac{\pi D_0^2}{4} \left(l - \frac{l}{0.988} + \frac{\Delta'_{g+m}}{0.988} \right). \quad (8)$$

From Bridgman's (1940) work, we find that ΔV_g at -10°C can be expressed in terms of the true pressure P and the initial volume V_g^0 as follows:

$$\Delta V_g = V_g^0 \left(5.650 \times 10^{-4} P - 7.235 \times 10^{-7} P^2 \right). \quad (9)$$

By substituting 1.27 cm for D_0 eq 4, 7, 8 and 9 reduce to the following expression for the true change in volume of the test specimen ΔV_s :

$$\Delta V_s = 1.282 \left(\Delta_{s+m} - \Delta'_{s+m} \right) + V_g^0 \left(5.650 \times 10^{-4} P - 7.235 \times 10^{-7} P^2 \right). \quad (10)$$

The results of the tests reported given in the relative volume V_s^P/V_s^0 versus true pressure P plane. The relative volume is found as follows:

$$V_s^P/V_s^0 = 1 - \Delta V_s/V_s^0. \quad (11)$$

where V_s^0 is the volume of the test specimen at atmospheric pressure and -10°C .

THE COMPRESSIBILITY OF ICE AT -10°C

Essential to the study of the compressibility of ice is a discussion of the phase diagram of water. Bridgman (1911, 1912, 1914, 1937) published several articles which are still the main source on the phase diagram of water and ice. Although the transition pressures in the phase diagram of water have been studied by others since 1937, these studies have been concerned with properties of water other than compressibility and specific density, the properties of main interest here.

Figure 9 illustrates the phase diagram of water as it is known today. This figure shows that the following transition will occur during the isothermal compressibility of ice at -10°C . At a pressure of 1.11 kbars ice I will melt to the liquid phase (water). If the pressure is raised further, the liquid phase will freeze to ice V at a pressure of 4.42 kbars. Upon continued pressure increase, ice V will undergo a polymorphic transition to ice VI at a pressure of 6.25 kbars. Finally ice VI will transform into ice VIII at a pressure of 20.8 kbars. The densities and the specific volumes of the various water phases at different temperatures and pressures may be extracted from Bridgman's data (1911, Tables XXV and XXX; and 1937, Table I).

The specific volume of ice I at 0°C and atmospheric pressure is given in Table III as $1.0900 \text{ cm}^3/\text{g}$. It is assumed that the coefficient of thermal expansion of ice I is small; therefore, the specific volume of ice I at -10°C is also $1.0900 \text{ cm}^3/\text{g}$. From the same table the specific volume of ice I and water at the transition point of 1.11 kbars and -10°C can be interpolated as 1.0664 and $0.9544 \text{ cm}^3/\text{g}$ respectively. Other points on the specific volume-pressure curve are determined below.

Table IV gives the specific volume of water and ice V at the transition points for various temperatures. The water-ice V transition at -10°C occurs at 4.42 kbars. At a temperature of -10°C

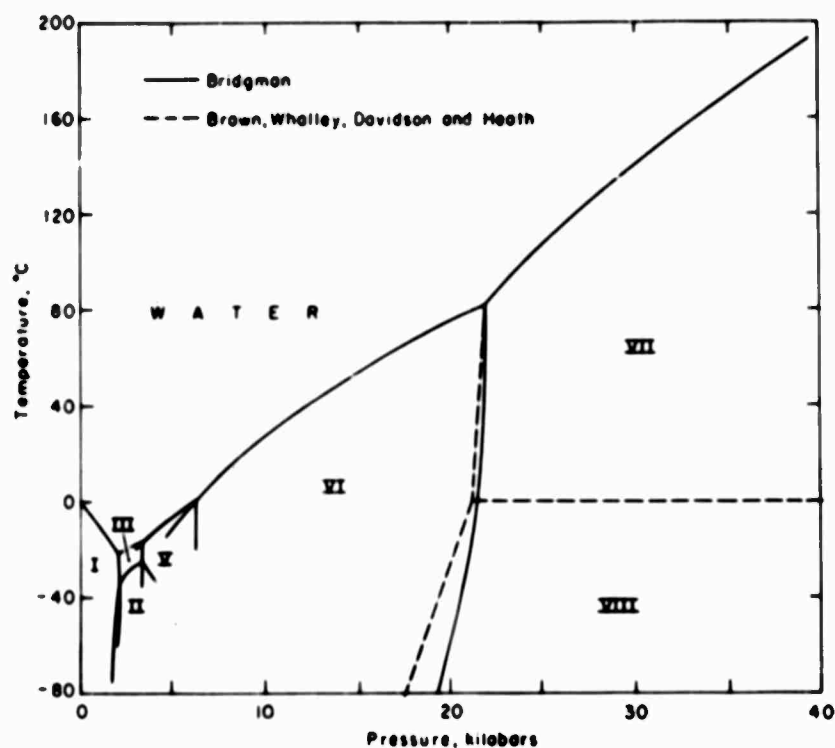


Figure 9. Phase diagram of water in the temperature-pressure plane.

Table III. Specific volume of water and ice I on the equilibrium curve*

Pressure (kg/cm ²)	Pressure (kbars) †	Temp. (°C)	Specific vol. of water (cm ³ /g)	Specific vol. change (cm ³ /g)	Specific vol. of ice (cm ³ /g)
0	0.0	0	1.0000	0.0900	1.0900
500	0.49	- 4.1	0.9777	.0998	1.0775
1000	0.98	- 8.7	0.9588	.1096	1.0684
1500	1.47	- 14.0	0.9414	.1201	1.0615
2000	1.96	- 20.3	0.9253	.1318	1.0571

* Bridgman, 1911, taken from Table XXX

† 1 kg cm⁻² = 0.98 × 10⁻¹ kbars

Table IV. Specific volume of water and ice V on the equilibrium curve*

Pressure (kg/cm ²)	Pressure (kbars) †	Temp. (°C)	Specific vol. of water (cm ³ /g)	Specific vol. change (cm ³ /g)	Specific vol. of ice (cm ³ /g)
3500	3.43	- 17.0	0.8870	0.0785	0.8085
4000	3.92	- 13.6	.8781	.0733	.8048
4500	4.41	- 10.1	.8694	.0681	.8013
5000	4.90	- 7.0	.8610	.0634	.7976
5500	5.39	- 4.2	.8543	.0590	.7953
6000	5.88	- 1.6	.8478	.0549	.7929
6500	6.37	+ 0.6	.8418	.0516	.7902

* Bridgman, 1911, taken from Table XXX

† 1 kg cm⁻² = 0.98 × 10⁻¹ kbars

Table V. Specific volume change on the ice V - ice VI equilibrium curve*

Pressure (kg/cm ²)	Pressure (kbars)	Temp. (°C)	Specific vol. change (cm ³ /g)
6365	6.24	-20.0	0.03809
6370	6.25	-15.0	.03828
6374	6.25	-10.0	.03847
6377	6.25	- 5.0	.03866
6381	6.25	0.0	.03886

* Bridgman, 1911; taken from Table XXV

† 1 kg/cm² = 0.98×10^{-3} kbars

Table VI. Specific volume change on the ice VI - ice VII equilibrium curve*

Pressure (kg/cm ²)	Pressure (kbars)†	Temp. (°C)	Specific vol. change (cm ³ /g)
22,000	21.6	- 0.0	0.0567
22,260	21.8	20.0	.0570
22,360	21.9	40.0	.0573

* Bridgman, 1937; taken from Table I

† 1 kg/cm² = 0.98×10^{-3} kbars

and a pressure of 4.42 kbars the specific volume of water is interpolated as 0.8688 cm³/g. At the same temperature and pressure the specific volume of ice V is interpolated as 0.8012 cm³/g.

From here on it becomes more difficult to find reliable data. Although Bridgman was most successful in obtaining the volume changes occurring at the phase changes, he had great difficulty measuring the compressibilities of the various phases of water. He did, however, develop specific volume data for ice and water along their equilibrium curves.

From the equilibrium data for the ice V - water transition (Table IV) it is possible to approximate the specific volume of ice V at -10°C. At a pressure of 6.25 kbars and a temperature of +0.2°C the specific volume of ice V is interpolated as 0.7907 cm³/g. It is assumed that changes in pressure have a much greater effect than changes in temperature on the specific volume of ice V. The volume change associated with the temperature difference of 10.2°C is neglected and the specific volume of ice V at 6.25 kbars and -10°C is assumed to be 0.7907 cm³/g. For the phase transition of ice V to ice VI at -10°C, Table V gives the change in volume as 0.03847 cm³/g. The specific volume of ice VI at -10°C and 6.25 kbars is thus 0.7907-0.0385 = 0.7522 cm³/g.

The volume of ice VIII at -10°C and 20.8 kbars is the next calculation to be made. Bridgman did not recognize this phase of ice but thought it to be ice VII. Ice VIII was first observed by Brown and Whalley (1966) and Whalley et al (1966), using dielectric techniques. They did not provide data for ice VIII. However, they did suggest that the volume change associated with the ice VII to ice VIII transition is very small ($0 \pm 2.78 \times 10^{-4}$ cm³/g at the ice VI-VII-VIII triple point).

With this in mind, we can approximate the volume of ice VIII. From Bridgman's work, we find that ice VII has a specific volume of approximately 0.60 cm³/g at room temperature and

Table VII. Compressibility of ice *

Phase	Pressure (kbars)	Specific vol. (cm ³ /g)	Relative vol.
Temperature -10C			
Ice I	0.0	1.0900	1.000
Ice I	1.11	1.0664	0.978
Water	1.11	0.9544	0.876
Water	4.42	0.8688	0.796
Ice V	4.42	0.8012	0.736
Ice V	6.25	0.7907	0.726
Ice VI	6.25	0.7522	0.690
Ice VI	20.8	0.702	0.644
Ice VIII	20.8	0.645	0.592
Ice VIII	49.1	0.60	0.55
Temperature +5C			
Water	0.0	0.9999	1.0000
Water	6.87	.8370	0.8370
Ice VI	6.87	.7488	0.7488
Ice VI	21.7	.702	0.702
Ice VIII	21.7	.645	0.645
Ice VIII	49.1	.60	0.60

* Calculated from experimental data reported by Bridgman (1911, 1937).

49.1 kbars. We assume that the temperature effect on the specific volume of ice VII is small in comparison with pressure effects. Furthermore, we assume that the volume change associated with the phase transition of ice VII to ice VIII is negligible and that ice VIII exhibits the same compressibility as ice VII. Thus, the specific volume of ice VIII at 49.1 kbars and -10C is 0.60 cm³/g. The volume change associated with a pressure increase from 19.6 to 44.1 kbars for ice VII is given by Bridgman (1937) as a mean value of 0.039 cm³/g. We assume that this value is representative in the pressure range of 20.8 to 49.1 kbars at -10C. The resulting volume change for ice VIII at -10C from 49.1 to 20.8 kbars is 0.045 cm³/g. The specific volume for ice VIII at -10C and 20.8 kbars is, thus, calculated to be $0.60 + 0.045 = 0.645$ cm³/g.

The volume change of ice VII to ice VI at the transition temperature of -10C and 21.4 kbars is extrapolated from Table VI to be 0.057 cm³/g. We assume that this value holds for the volume change of ice VIII to ice VI at -10C and 20.8 kbars. The resulting specific volume for ice VI at -10C and 20.8 kbars is $0.645 + 0.057 = 0.702$ cm³/g. This completes the calculations for the compressibility of ice at -10C from 0 to 49.1 kbars. The results are tabulated in Table VII and illustrated in Figure 10. The compressibility of each phase is assumed to be linear.

Similar calculations can be performed at other temperatures. In Figure 10, the compressibility of water at +5C is plotted along with the compressibility of ice at -10C. Ice is more compressible than water; therefore, saturated frozen ground would be expected to be more compressible than saturated unfrozen ground.

Figures 11 through 13 and Tables AI-ALII, Appendix A, give test results for the isothermal compressibility of ice. The compressibility as predicted from Bridgman's data is plotted for comparison. The variation of the test results from Bridgman's results can be attributed primarily to rate effects. Bridgman (1911) reported that the change in the volume of the phase changes was

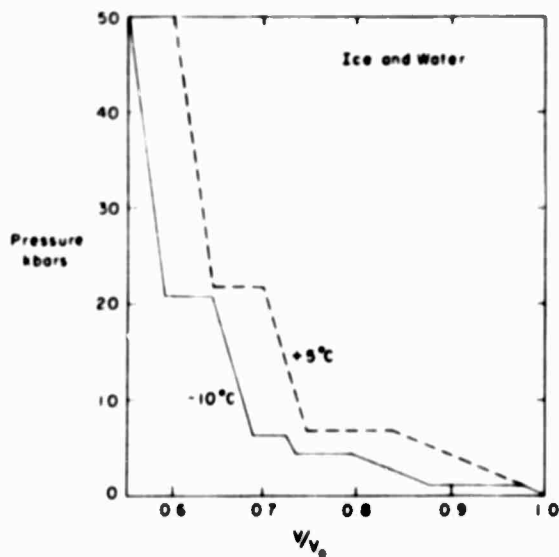


Figure 10. Predicted isothermal compressibility of ice at -10°C and water at $+5^{\circ}\text{C}$.

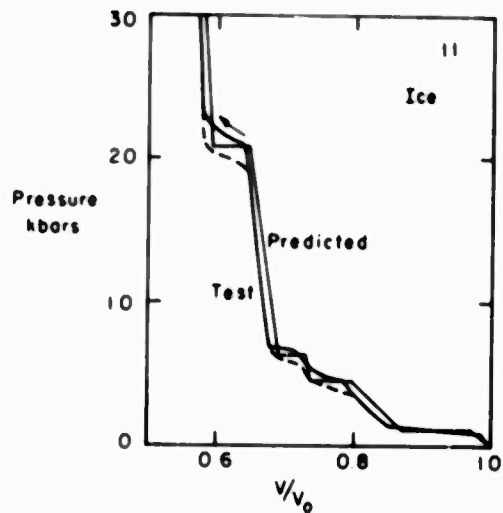


Figure 11. Isothermal compressibility of ice, specimen 11.

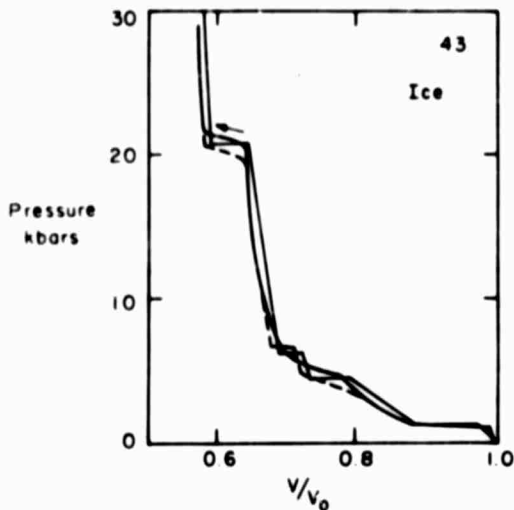


Figure 12. Isothermal compressibility of ice, specimen 43.

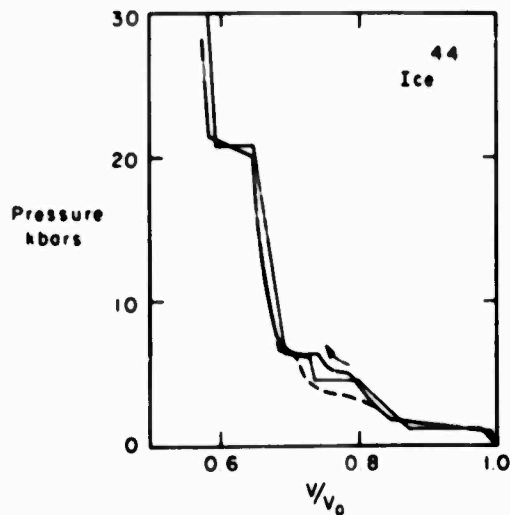


Figure 13. Isothermal compressibility of ice, specimen 44.

time dependent; e.g., the time for completion of the liquid-solid reaction was about two hours on the ice I-liquid boundary. The solid-solid reactions were nearly explosive near the triple point but were slow at other points. The time allotted for the tests reported here (≈ 40 min/cycle) was probably inadequate to allow complete phase transformations at the transition pressures.

The slightly greater compressibility of the results reported might be explained by the presence of microscopic air bubbles. An included air volume of approximately 1% would account for the differences.

Bridgman (1911) found that ice V nucleated only in the presence of glass splinters. Two of the three ice specimens tested showed the liquid-ice V transition. However, for specimen 43 (Fig 12) ice V did not nucleate and the liquid phase froze to ice VI upon loading beyond the liquid-ice V transition. In all tests ice V was observed on the unloading cycle; this is consistent with Bridgman's results.

THE COMPRESSIBILITY OF FROZEN SAND AND SILT AT -10°C

The results of the isothermal compressibility tests on frozen sand and silt are given in Appendix A and in Figures 14-28.

It was suggested in the introduction that only a few material properties were needed to estimate the compressibility of frozen ground. This problem has been discussed by Brace (1965) and Stephens (1964) for rocks. The general approach has been to average the compressibilities of the minerals making up the rock. Two kinds of averages have been employed: the Reuss average

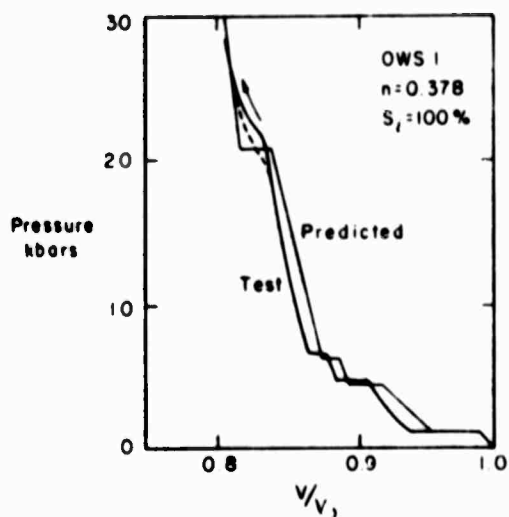


Figure 14. Isothermal compressibility of fully saturated Ottawa banding sand, specimen 1.

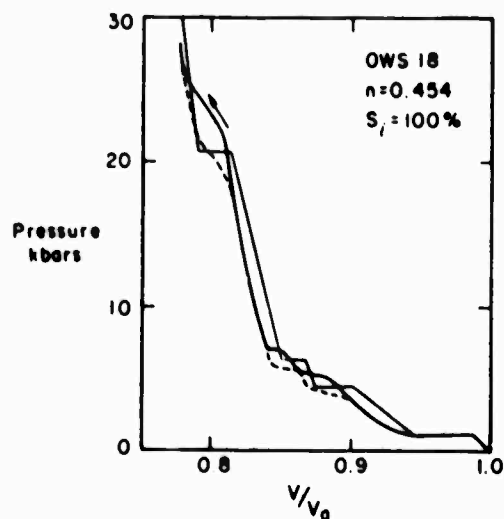


Figure 15. Isothermal compressibility of fully saturated Ottawa banding sand, specimen 18.

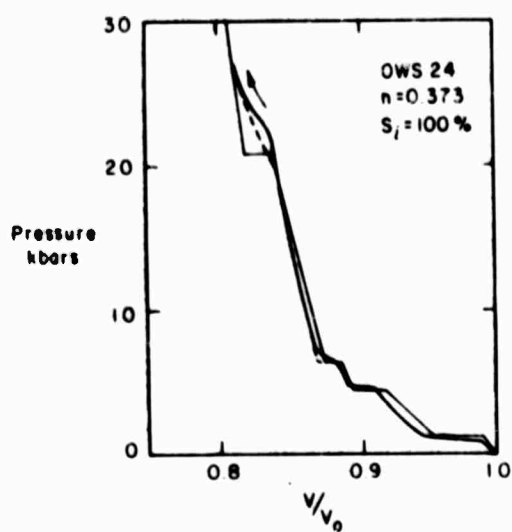


Figure 16. Isothermal compressibility of fully saturated Ottawa banding sand, specimen 24.

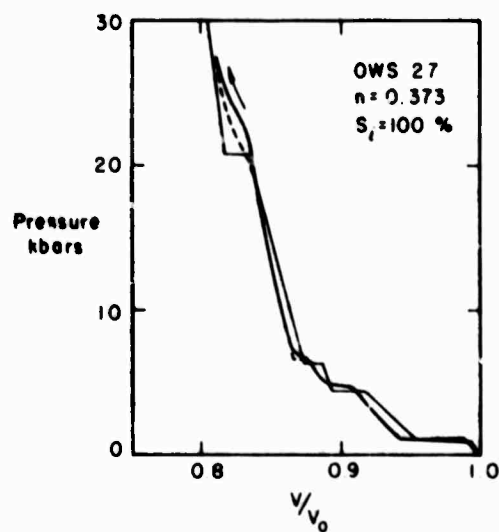


Figure 17. Isothermal compressibility of fully saturated Ottawa banding sand, specimen 27.

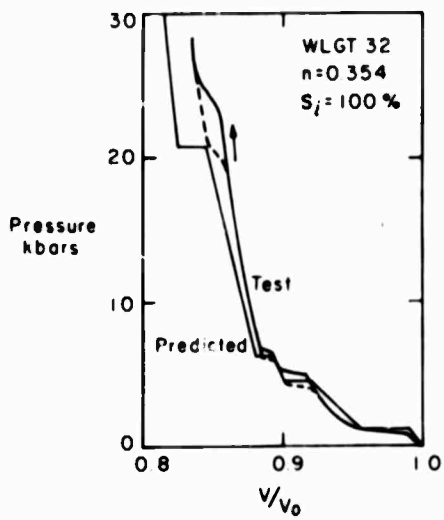


Figure 18. Isothermal compressibility of fully saturated West Lebanon glacial till, specimen 32.

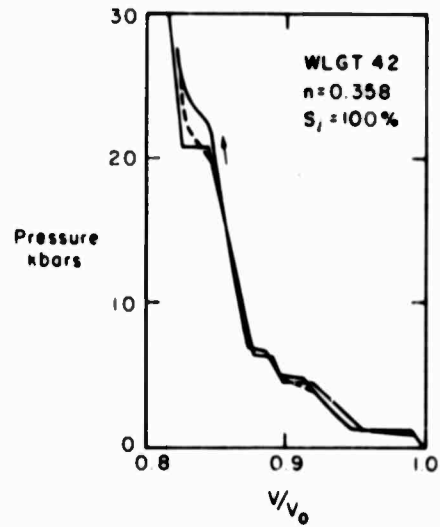


Figure 19. Isothermal compressibility of fully saturated West Lebanon glacial till, specimen 42.

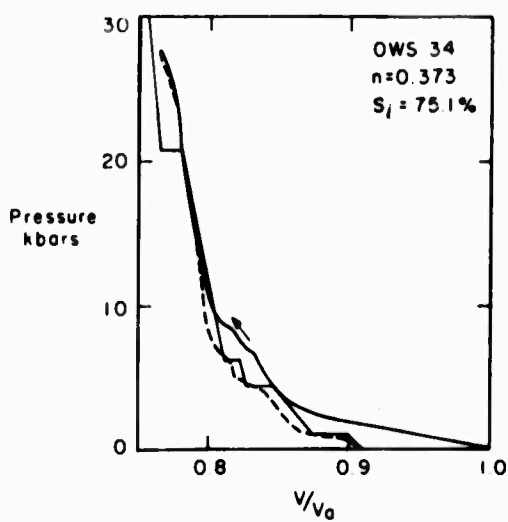


Figure 20. Isothermal compressibility of partially saturated Ottawa banding sand, specimen 34.

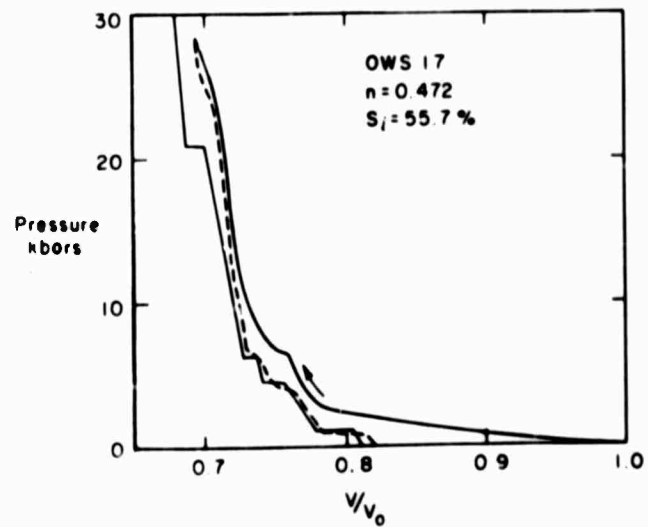


Figure 21. Isothermal compressibility of partially saturated Ottawa banding sand, specimen 17.

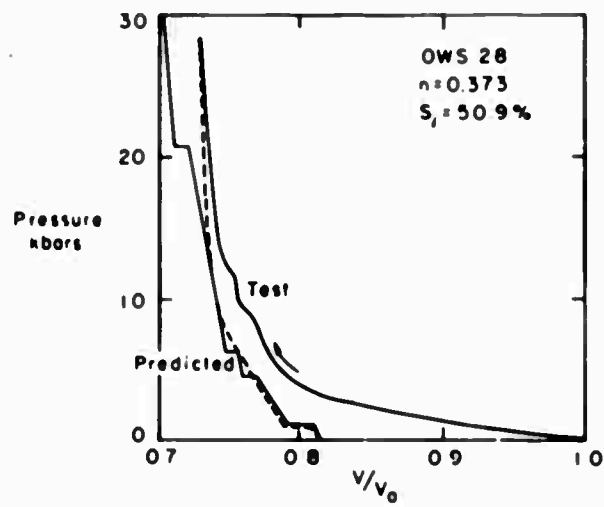


Figure 22. Isothermal compressibility of partially saturated Ottawa banding sand, specimen 28.

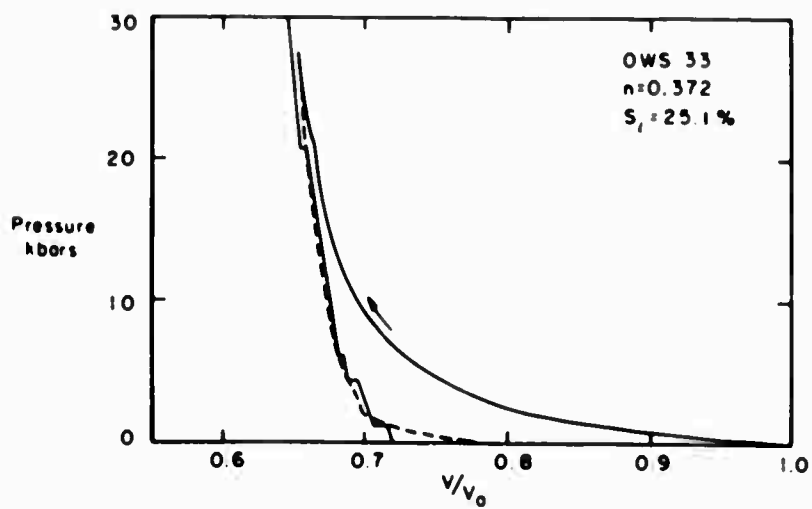


Figure 23. Isothermal compressibility of partially saturated Ottawa banding sand, specimen 33.

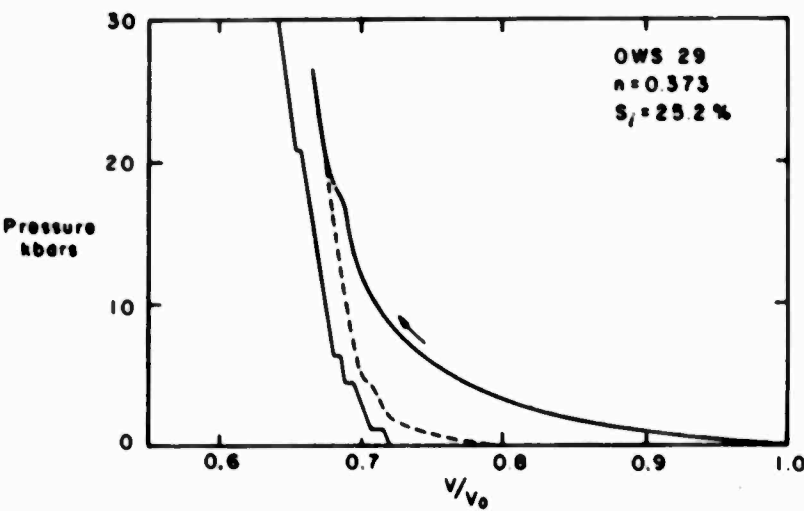


Figure 24. Isothermal compressibility of partially saturated Ottawa banding sand, specimen 29.

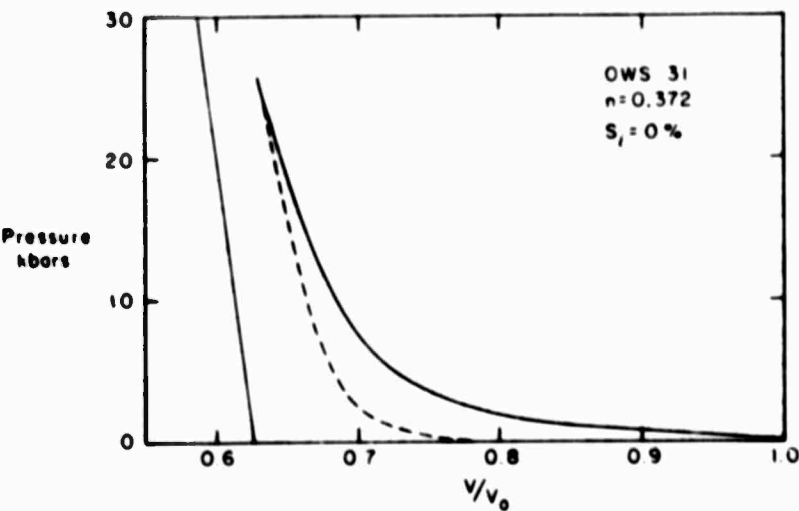


Figure 25. Isothermal compressibility of dry Ottawa banding sand, specimen 31.

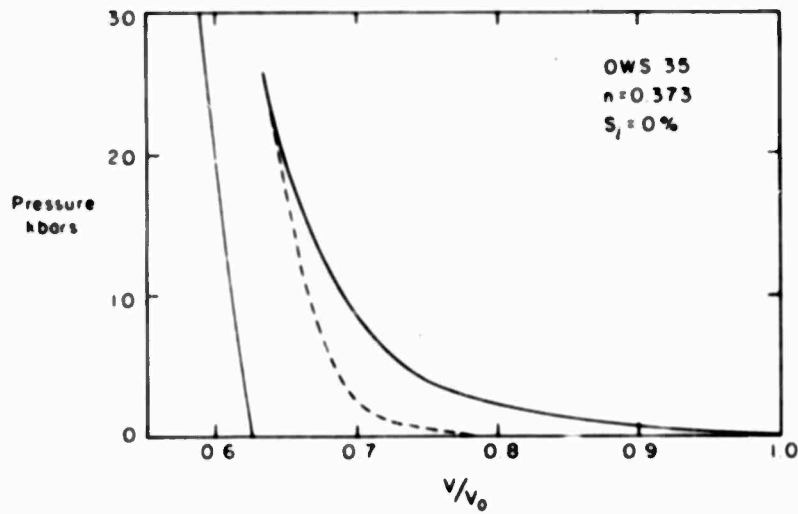


Figure 26. Isothermal compressibility of dry Ottawa banding sand, specimen 35.

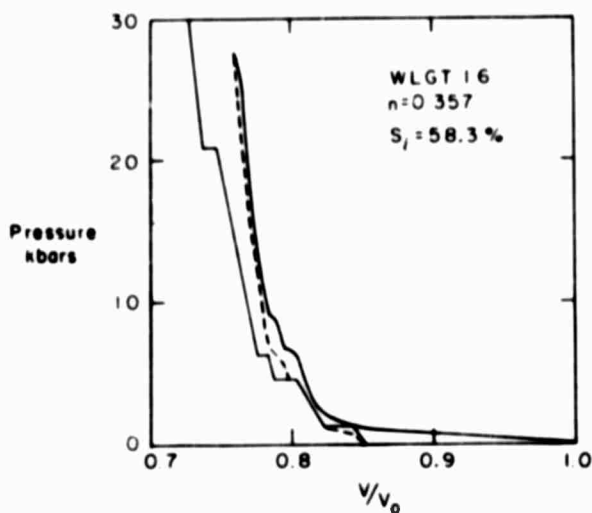


Figure 27. Isothermal compressibility of partially saturated West Lebanon glacial till, specimen 16.

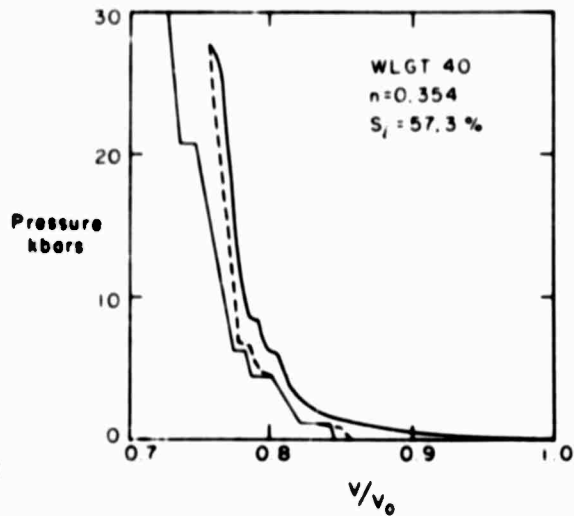


Figure 28. Isothermal compressibility of partially saturated West Lebanon glacial till, specimen 40.

and the Voigt average. The Reuss average B_r is given by:

$$B_r = V_a B_a + V_b B_b + V_c B_c + \dots \quad (12)$$

where V_a , V_b , etc. are volume percentages of the minerals in the rock, and B_a , B_b , etc. are the volume compressibilities of the minerals. The Reuss average provides an upper bound. The lower bound, the Voigt average B_v is given by:

$$1/B_v = V_a/B_a + V_b/B_b + V_c/B_c + \dots \quad (13)$$

The Russ averaging method assumes uniform distribution of stress throughout the matrix and neglects the difficulty in fitting the distorted grains together. The Voigt model assumes a uniform strain throughout the matrix and neglects the non-equilibrium stress conditions that exist. If discrepancies occurred between the predicted compressibilities given by eq 12 and 13 and the measured values, porosity or alterations of the minerals in the rock were listed as causes.

The prediction of the compressibility of frozen soil is analogous to that of rock. Fully and partially saturated frozen ground are discussed separately.

THE COMPRESSIBILITY OF FULLY SATURATED FROZEN GROUND

A saturated frozen ground can be considered as a rock made up of two components: ice and mineral particles. The compressibility of saturated frozen ground can be estimated by either eq 12 or 13 if we assume that the ice flows plastically. The problem is complicated by the phase transitions that ice undergoes when compressed to 30 kbars at -10°C . This fact precludes the direct use of eq 12 or 13. A consequence of eq 12 is that the total volume change ΔV_s is the mere sum of the volume changes in the component materials, the mineral particles ΔV_m and the ice ΔV_i ; i.e.

$$\Delta V_s = \Delta V_m + \Delta V_i. \quad (14)$$

With knowledge of ΔV_m and ΔV_i , ΔV_s can thus be computed at any pressure and temperature. Values for ΔV_m can be obtained from data given by Brace (1965), Stephens and Lilley (1966), and Stephens (1964).

A general equation for the compressibility of frozen ground, with porosity as the main parameter, can now be derived. Porosity n is defined as the ratio of the volume of voids V_v^0 to the total volume V_s^0 at atmospheric pressure:

$$n = V_v^0 / V_s^0. \quad (15)$$

For a porous medium saturated with ice, eq 15 becomes:

$$n = V_i^0 / V_s^0 \quad (16)$$

where V_i^0 is the volume of ice at atmospheric pressure.

ΔV_i at pressure P is given by:

$$\Delta V_i = n V_s^0 (1 - v_i^p / v_i^0) \quad (17)$$

where v_i^p / v_i^0 is the value that can be obtained from Table VII, at any pressure. The volume of the mineral solids V_m^0 is:

$$V_m^0 = V_s^0 - V_i^0 \quad (18)$$

and ΔV_m is given by

$$\Delta V_m = (V_m^0 - V_m^p) (aP - bP^2) \quad (19)$$

where a and b are compressibility coefficients and P is pressure in kbars. Values for a range from 2.68×10^{-1} for quartz to 1.01×10^{-1} for augite (Brace, 1965). Values for b range from 24×10^{-4} for quartz to 3.9×10^{-4} for calcite.

The total volume change caused by pressure P is given by:

$$\Delta V_s = nV_s^0 \left(1 - v_i^p/v_i^0 \right) + (V_s^0 - V_i^0)(aP - bP^2). \quad (20)$$

The relative volume ratio V_i^p/V_i^0 is usually plotted versus P . Thus

$$V_i^p/V_i^0 = \Delta V_s/V_s^0 = 1 - n \left(1 - v_i^p/v_i^0 \right) - (1 - n) + (aP + bP^2). \quad (21)$$

Figures 14-19 show the compressibilities of saturated frozen Ottawa banding sand and West Lebanon glacial till with the predicted compressibilities. The compressibilities for ice obtained from Bridgman's work are used for the prediction. Other than in the regions of the phase changes, the differences are subtle. The differences noted at the phase changes are of the same nature as those observed for pure ice. However, the ice VI-ice VIII transition appears to begin at a higher pressure than expected (22.5 kbars vs 20.8 kbars). This again may be the result of the time-dependent behavior of the reaction. But it may also be caused by a nonhomogeneous pressure distribution; i.e., the time is not sufficient for the pressure on the mineral component and that on the ice to equilibrate so the mineral component takes a higher pressure.

THE COMPRESSIBILITY OF PARTIALLY SATURATED FROZEN GROUND

By definition, unsaturated frozen ground consists of a mineral phase, a gas phase, and an ice phase. The degree of saturation S_i is defined as the ratio of the volume of the voids filled with ice V_i^0 and the total voids volume V_v^0 . Thus

$$V_i^0 = S_i V_v^0. \quad (22)$$

V_i^0 can be expressed in terms of the total volume V_s^0 and the porosity n by

$$V_i^0 = S_i n V_s^0. \quad (23)$$

In an analogy with our analysis for saturated frozen ground, the changes in the volume of unsaturated frozen ground can be written as the sum of the true change in the volume of the mineral material ΔV_m , of the ice ΔV_i and of the air voids ΔV_a . Thus

$$\Delta V_s = \Delta V_m + \Delta V_i + \Delta V_a. \quad (24)$$

In a partially saturated soil, the volume of the air voids V_a^0 is given by

$$V_a^0 = (1 - S_i) V_v^0 = (1 - S_i) n V_s^0. \quad (25)$$

We will assume for now that all voids close with slight pressure. Then

$$\Delta V_s = V_s^0 = (1 - S_i) n V_s^0. \quad (26)$$

In an analogy with eq 17, the volume change of the ice at any pressure in an unsaturated frozen ground is given by

$$\Delta V_i = S_i n V_s^0 (i - v_i^p/v_i^0) \quad (27)$$

and ΔV_m is given by

$$\Delta V_m = (V_s^0 - V_v^0) (aP + bP^2) \quad (28)$$

Hence

$$\Delta V_s = (1 - S_i) n V_s^0 + S_i n V_s^0 (i - v_i^p/v_i^0) + (V_s^0 - V_v^0) (aP + bP^2), \quad (29)$$

and

$$V_s^p/V_s^0 = i - \Delta V_s/V_s^0 = 1 - (1 - S_i) n - S_i n (i - v_i^p/v_i^0) - (i - n) (aP + bP^2). \quad (30)$$

The isothermal compressibility of unsaturated frozen ground is thus a function of the degree of saturation with ice S_i , the porosity n , and the isothermal compressibility of ice and mineral particles.

In Figures 20-28, the results for the compressibility of partially saturated Ottawa banding sand and West Lebanon glacial till are plotted with the predicted compressibility. The values used for a and b in eq 30 were 2.68×10^{-3} and 24×10^{-6} ; P was in kbars. Specimens with various degrees of saturation were tested.

For the partially saturated ($S_i = 58\%$) West Lebanon glacial till (Fig 27 and 28) it appears that the air void closure occurred at some pressure below 2 kbars. The air void closure as observed is somewhat complicated and is partially obscured by the phase change that occurs at 1.11 kbars. The predicted compressibility is plotted for comparison. At the higher pressures there appears to be some deviation of the test results from the predicted values. Moreover, on the loading cycle the phase changes nucleate at a higher pressure than predicted. This occurrence indicates that complete air void closure has not taken place or, what is more likely, that the mineral component is subjected to a greater stress than the ice. This behavior is undoubtedly dependent upon the rate of compression.

The compressibilities for partially saturated Ottawa banding sand are plotted in Figures 20-26. Again the predicted values are shown for comparison. It appears that the air void closure is not obtained at 2 kbars. For 75% and 50% saturated specimens closure does not appear to occur until approximately 10 kbars. The phase changes are not well defined nor do they appear to be complete. Again, the phase changes nucleate at higher pressures than predicted. On the unloading curves the phase changes appear as predicted, although the rate dependence is still in evidence. The difference between the test results and the predicted values for the compressibilities of partially saturated sand is small (approximately 1% of the initial volume). This difference is well within the experimental accuracy.

It can be observed in the loading curves that a significant pressure is required to close the air voids. The prediction of the closure of the air voids as a function of pressure appears to be difficult.

The compressibility of rocks with small cracks or with spherical pores was investigated by Walsh (1965 a,b). He investigated analytically the elastic behavior of solids with cracks running through them. Important parameters are the shape and direction of the crack. Small differences

in crack length with direction could lead to significant differences in linear compressibility. According to Walsh, the hydrostatic pressure necessary to close an elliptic cavity is

$$P = E a \quad (31)$$

where E is Young's modulus and a is the ratio of minor to major radius of the cavity. A spherical cavity requires a larger pressure for closure. Equation 31 applies to a dry homogeneous rock, or to a dry nonhomogeneous rock if E is the Young's modulus of the weakest material. Equation 31 also assumes that the cavity is closed by elastic deformation. If the crack is closed by plastic flow or by brittle failure, eq 31 does not apply.

On the other hand, partially saturated frozen ground consists of ice and an unconsolidated mineral matrix. The first reduction in air void volume would occur not by elastic deformation or by plastic flow but by rearrangement of the mineral particles. This would be followed or accompanied by crushing of the individual particles. The extent of the rearrangement and the crushing would be governed by the amount of ice present. As the mineral particles are being rearranged and crushed, the ice would flow plastically. At some pressure the ice would completely fill the voids and be subjected to the same overall pressure as the particles. The compressibility then would be governed by the deformation of the mineral particles and the plastic deformation of the ice.

The pressure at which the air voids close is influenced by the degree of saturation with ice. The air voids in soils with a high degree of saturation would close at a relatively low pressure while those with a low degree of saturation would require a higher pressure for air void closure. Moreover, the rearrangement and crushing may be expected to be more efficient for a wet soil than for a dry soil.

The Ottawa sand specimen 33 (Fig. 23), with a 25% saturation, exhibits a somewhat different behavior from that of the specimens with higher degrees of saturation. Closure does not appear to occur until a pressure of approximately 20 kbars has been reached. Upon unloading, the test data follow the predicted data down to a pressure of approximately 1 kbar. The phase changes are not well defined. This would be expected because of the small volume of ice present. However, at approximately 1 kbar, the test data leave the predicted values and the specimen appears to expand elastically. Figures 25 and 26 show that the dry Ottawa sand specimens have the same elastic expansion for the low-pressure release curve. In fact, the dry and 25% saturated specimens release to approximately the same relative volume (0.78). This relative volume is the smallest volume regardless of the degree of saturation to which Ottawa banding sand can be compressed under the test conditions.

The Ottawa banding sand compressibility curves look much like those reported for dry Monterey sand by Stephens and Lilley (1966). Complete closure of the voids is not obtained and the mineral particles deform elastically.

To test the validity of the methods used in reducing the raw data for the partially saturated soils, the first and second compressibilities were calculated for a fully saturated sand. The results of this comparison (Fig. 29) indicate that the methods used to reduce the data from the first compression are valid. However, the phase transition of ice I to water is somewhat obscured and the subsequent phase transitions occur at somewhat high pressures than expected.

The results of three compression cycles on dry Ottawa banding sand are illustrated in Figure 30. This figure shows that the voids undergo maximum closure during the first compression. The first release curve and the additional compression cycles follow nearly the same path. Thus, it appears that the working of the mineral particles and the subsequent breakdown do not result in a further change in compressibility.

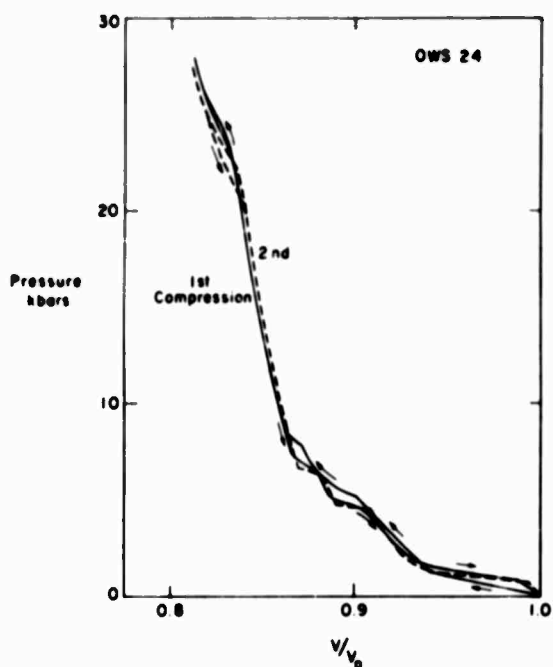


Figure 29. First and second compressibilities of fully saturated Ottawa banding sand, specimen 24.

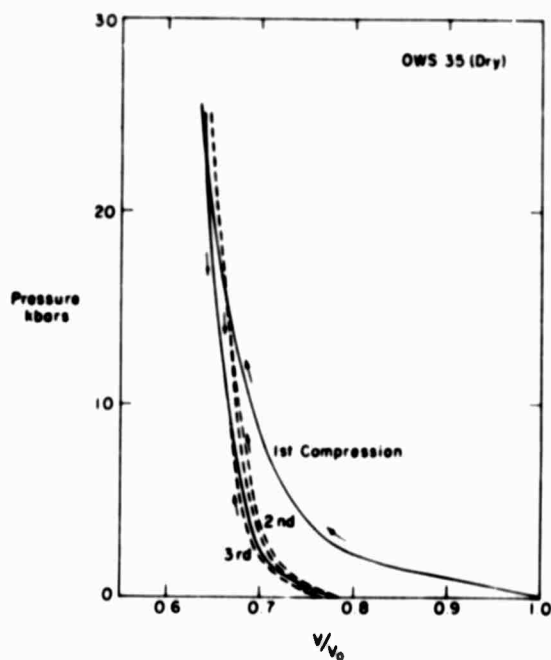


Figure 30. First, second and third compressibilities of dry Ottawa banding sand, specimen 35.

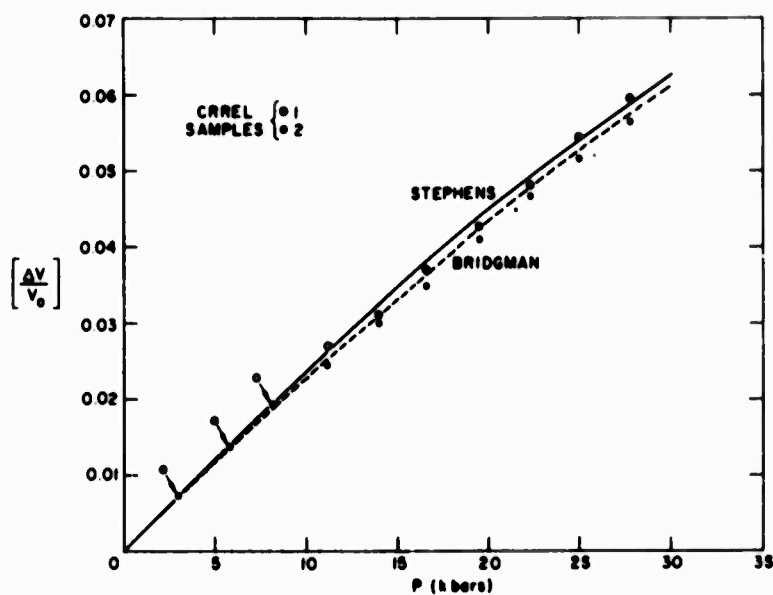


Figure 31. The isothermal compressibility of indium.

The isothermal compressibility of indium was determined as an additional check on the accuracy of our procedures and equipment. The procedures followed were identical to those used for the compressibility of the frozen sand, frozen silt, and ice. The compressibility of indium was compared with that of gold. The results are given in Figure 31. Results obtained by Bridgman (1935) and Stephens (1967) are shown for comparison.

CONCLUSIONS

The compressibility of frozen soil is readily predicted from the knowledge of material properties such as the degree of saturation with ice, the porosity, and the compressibilities of the ice and mineral components. The behavior of the phase transitions for partially saturated frozen soils is somewhat obscured by the rearrangement and crushing of the mineral particles. Materials with no ice or a low degree of saturation demonstrate elastic rebound on the release leg of the compression cycle. Apparently there is a maximum dry density to which a particular soil can be compressed, and this density is somewhat less than that of the voidless mineral parent.

The compressibility of ice is as predicted by Bridgman (1911, 1937). However, time-dependent behavior is demonstrated for the phase transitions. Complete phase transitions were not observed at constant pressure.

The compressibilities in the low-pressure region (below 2 kbars) were not well defined. This is primarily a result of the test method. A technique employing a liquid cell in the low-pressure region is being pursued and the results will be reported later.

LITERATURE CITED

- Adams, L.H. and Williamson, E.D. (1923) On the compressibility of minerals and rocks at high pressures. *Journal of the Franklin Institute*, vol. 195, p. 475-525.
- Bassett, W.A.; Takahashi, Taro; Mao, Ho-Kwang and Weaver, J. Scott. (1968) Pressure-induced phase transformation in NaCl. *Journal of Applied Physics*, vol. 39, no. 1.
- Brace, W.F. (1965) Some new measurements of linear compressibility of rocks. *Journal of Geophysical Research*, vol. 70, no. 2, p. 391-397.
- Bridgman, P.W. (1911) Water in the liquid and five solid forms, under pressure. *Proceedings of the American Academy of Arts and Sciences*, vol. 47, p. 441-558.
- (1912) Thermodynamic properties of liquid water to 80° and 12,000 kgm. *Proceedings of the American Academy of Arts and Sciences*, vol. 48, p. 309-362.
- (1914) High pressures and five kinds of ice. *Journal of the Franklin Institute*, vol. 177, p. 315-332.
- (1937) The phase diagram of water to 45,000 kg/cm². *Journal of Chemical Physics*, vol. 5, p. 964-966.
- (1940) The compression of 46 substances to 50,000 kg/cm². *American Academy of Arts and Sciences*, vol. 74, p. 21-51.
- (1964) *Collected experimental papers*. Cambridge, Mass. Harvard University Press, 7 vols.

LITERATURE CITED (Cont'd)

- Brown, A.J. and Whalley, E. (1966) Preliminary investigation of the phase boundaries between ice VI and VII and ice VIII. *Journal of Chemical Physics*, vol. 45, p. 4360-4361.
- Brown, Wayne; DeVries, K.L. and Smith, J.L. (1967) Properties of rock tested in one-dimensional compression. Air Force Weapons Laboratory, AFWL-TR-66-124.
- Pauiding, B.W.; Cornish, R.H.; Abbott, B.W. and Finlayson, L.A. (1965) Behavior of rocks and soils under high pressure. Air Force Weapons Laboratory, AFWL-TR-65-51.
- Stephens, D.R. (1934) The hydrostatic compression of eight rocks. *Journal of Geophysical Research*, vol. 69, no. 14, p. 2967-2977.
- _____ and Lilley, E.M. (1966) Static PV curves of cracked and consolidated earth materials to 40 kb. University of California, Lawrence Radiation Laboratory, UCRL-14711.
- _____ and Lilley, E.M. (1967) Procedure for pressure-volume runs on rocks. University of California, Lawrence Radiation Laboratory, UCID-15070.
- Walsh, J.B. (1965a) The effect of cracks on the compressibility of rock. *Journal of Geophysical Research*, vol. 70, no. 2, p. 381-389.
- Walsh, J.B. (1965b) The effect of cracks on the uniaxial elastic compression of rocks. *Journal of Geophysical Research*, vol. 70, no. 2, p. 399-411.
- Whalley, E.; Davidson, D.W. and Heath, J.B.R. (1966) Dielectric properties of ice VII, ice VIII: a new phase of ice. *Journal of Chemical Physics*, vol. 45, no. 11, p. 3976-3982.
- Wilson, G.J.; Chan, R.K.; Davidson, D.W. and Whalley E. (1965) Dielectric properties of ices II, III, V, and VI. *Journal of Chemical Physics*, vol. 43, no. 7, p. 2384-2391.

Table AIII. Isothermal compressibility of polycrystalline ice specimen 44.

Pressure kbars	Volume cm ³	Relative Volume
0.00	2.8880	1.0000
1.00	2.8632	0.9931
1.50	2.5387	0.8806
1.88	2.4361	0.8450
2.38	2.3932	0.8301
3.76	2.3107	0.8015
5.01	2.2329	0.7814
5.14	2.2113	0.7670
5.64	2.1666	0.7515
6.24	2.1394	0.7407
6.39	2.0349	0.7058
6.64	1.9977	0.6929
7.52	1.9595	0.6797
8.15	1.9456	0.6749
10.03	1.9259	0.6680
12.53	1.9047	0.6607
15.04	1.8868	0.6545
17.54	1.8676	0.6478
20.13	1.8534	0.6429
21.66	1.6744	0.5808
25.06	1.6651	0.5776
27.57	1.6526	0.5732
28.32	1.6519	0.5730
27.57	1.6526	0.5732
25.06	1.6651	0.5776
21.66	1.6744	0.5808
20.13	1.8534	0.6429
17.54	1.8676	0.6478
15.04	1.8868	0.6545
12.53	1.9047	0.6607
10.03	1.9259	0.6680
8.15	1.9456	0.6749
7.52	1.9595	0.6797
6.64	1.9977	0.6929
6.39	1.9706	0.6835
6.37	2.0579	0.7138
4.59	2.0859	0.7235
3.76	2.1871	0.7586
3.13	2.3101	0.8013
2.38	2.4060	0.8345
1.88	2.4515	0.8503
1.30	2.4987	0.8667
1.00	2.6734	0.9273
0.50	2.7926	0.9686
0.00	2.8652	0.9938

Table AII. Isothermal compressibility of polycrystalline ice specimen 43.

Pressure kbars	Volume cm ³	Relative Volume
0.00	2.7640	1.0000
0.73	2.7384	0.9907
1.25	2.4495	0.8862
1.38	2.4047	0.8700
1.68	2.3680	0.8549
2.51	2.2846	0.8266
3.31	2.2234	0.8062
4.79	2.1504	0.7730
5.26	2.0564	0.7368
6.27	1.9357	0.7014
7.52	1.8942	0.6853
10.03	1.8487	0.6689
12.53	1.8259	0.6606
15.04	1.8073	0.6539
17.54	1.7917	0.6432
19.30	1.7813	0.6445
20.68	1.7726	0.6413
21.03	1.7182	0.6216
21.30	1.6492	0.5967
21.91	1.6048	0.5806
22.56	1.6032	0.5800
25.06	1.5931	0.5764
27.57	1.5374	0.5743
29.02	1.5065	0.5718
29.45	1.6131	0.5836
30.05	1.7150	0.6205
19.30	1.7590	0.6364
17.54	1.7917	0.6432
15.04	1.8073	0.6539
12.53	1.8259	0.6606
10.03	1.8487	0.6689
7.52	1.8728	0.6776
6.69	1.8337	0.6715
6.64	1.9500	0.7164
4.59	2.0043	0.7253
3.76	2.1490	0.7775
3.31	2.2234	0.8062
2.51	2.2846	0.8266
1.68	2.3680	0.8549
1.33	2.4047	0.8700
1.25	2.4495	0.8862
0.78	2.7334	0.9907
0.00	2.7640	1.0000

Table AI. Isothermal compressibility of polycrystalline ice specimen 11.

Pressure kbars	Volume cm ³	Relative Volume
0.00	2.6500	1.0000
0.75	2.6152	0.9869
1.00	2.5100	0.9472
1.25	2.3309	0.8796
1.43	2.2666	0.8553
2.76	2.1711	0.8193
3.76	2.1197	0.7999
4.51	2.0796	0.7848
4.76	2.0289	0.7656
5.51	1.9528	0.7369
6.52	1.8953	0.7152
6.77	1.7983	0.6786
7.52	1.7914	0.6760
10.03	1.7680	0.6672
12.53	1.7478	0.6595
17.54	1.7190	0.6487
19.05	1.7068	0.6441
19.80	1.7017	0.6422
20.30	1.6974	0.6405
21.05	1.6871	0.6367
21.81	1.5944	0.6017
22.56	1.5476	0.5840
24.31	1.5323	0.5782
27.57	1.5243	0.5752
30.08	1.5156	0.5719
22.56	1.5344	0.5790
21.81	1.5351	0.5793
21.05	1.5389	0.5807
20.30	1.5656	0.5908
19.80	1.6638	0.6279
19.05	1.7068	0.6441
17.54	1.7190	0.6487
12.53	1.7478	0.6595
10.03	1.7680	0.6672
7.52	1.7914	0.6760
6.76	1.7983	0.6786
6.52	1.8047	0.6810
5.51	1.9182	0.7238
4.76	1.9550	0.7302
4.51	1.9445	0.7338
3.76	2.1197	0.7999
2.76	2.1711	0.8193
1.43	2.2666	0.8553
1.25	2.3309	0.8796
1.00	2.5110	0.9472
0.75	2.6152	0.9869
0.00	2.6500	1.0000

Table AIV. Isothermal compressibility of Ottawa banding sand specimen 31.

$\alpha = 0.372$ $S_1 = 0\%$

Pressure kbars	Volume cm ³	Relative Volume
0.00	2.7220	1.0000
1.25	2.5339	0.9342
1.75	2.3447	0.8614
2.51	2.2130	0.8130
3.76	2.1372	0.7772
5.01	2.0665	0.7539
6.27	1.9933	0.7323
7.52	1.9243	0.7070
10.03	1.8742	0.6806
12.53	1.8366	0.6747
15.04	1.8086	0.6682
17.54	1.7839	0.6634
20.05	1.7641	0.6588
22.56	1.7445	0.6549
25.06	1.7287	0.6511
27.56	1.7160	0.6481
30.06	1.7045	0.6459
32.56	1.6949	0.6442
35.06	1.6861	0.6429
37.56	1.6785	0.6420
40.06	1.6719	0.6413
42.56	1.6661	0.6409
45.06	1.6611	0.6405
47.56	1.6568	0.6402
50.06	1.6531	0.6400
52.56	1.6499	0.6398
55.06	1.6471	0.6396
57.56	1.6447	0.6394
60.06	1.6425	0.6392
62.56	1.6404	0.6390
65.06	1.6385	0.6388
67.56	1.6367	0.6386
70.06	1.6350	0.6384
72.56	1.6334	0.6382
75.06	1.6319	0.6380
77.56	1.6304	0.6378
80.06	1.6290	0.6376
82.56	1.6276	0.6374
85.06	1.6263	0.6372
87.56	1.6250	0.6370
90.06	1.6238	0.6368
92.56	1.6226	0.6366
95.06	1.6214	0.6364
97.56	1.6203	0.6362
100.06	1.6192	0.6360

Table AV. Isothermal compressibility of Ottawa banding sand specimen 35.

$\alpha = 0.373$ $S_1 = 0\%$

COMPRESSION No. 1			COMPRESSION No. 2			COMPRESSION No. 3		
Press.	Vol.	Rel.	Press.	Vol.	Rel.	Press.	Vol.	Rel.
kbars	cm ³	Vol.	kbars	cm ³	Vol.	kbars	cm ³	Vol.
0.00	2.7220	1.0000	0.00	2.1333	0.7845	0.00	2.0803	0.7644
0.63	2.5339	0.9342	0.25	2.0834	0.7654	0.53	2.0019	0.7354
1.25	2.3447	0.8614	0.50	2.0518	0.7538	0.95	1.9633	0.7213
1.88	2.2130	0.8130	1.25	1.9901	0.7311	1.50	1.9264	0.7077
2.51	2.1372	0.7772	2.51	1.9378	0.7119	2.46	1.8929	0.6954
3.76	2.0665	0.7539	5.01	1.8875	0.6934	3.88	1.8637	0.6847
5.01	1.9933	0.7323	7.52	1.8629	0.6844	5.01	1.8485	0.6791
7.52	1.9243	0.7070	10.03	1.8444	0.6776	7.52	1.8273	0.6713
10.03	1.8742	0.6806	12.53	1.8266	0.6711	10.03	1.8109	0.6653
12.53	1.8366	0.6747	15.04	1.8116	0.6655	12.53	1.7963	0.6599
15.04	1.8086	0.6682	17.54	1.7900	0.6609	15.04	1.7804	0.6544
17.54	1.7839	0.6634	20.05	1.7865	0.6563	17.54	1.7694	0.6500
20.05	1.7641	0.6588	22.56	1.7726	0.6512	20.05	1.7589	0.6462
22.56	1.7445	0.6549	25.06	1.7590	0.6462	22.56	1.7484	0.6423
25.06	1.7287	0.6511	27.56	1.7582	0.6406	25.06	1.7381	0.6385
27.56	1.7160	0.6481	30.06	1.7501	0.6346	27.56	1.7284	0.6348
30.06	1.7045	0.6459	32.56	1.8208	0.6639	30.06	1.7189	0.6309
32.56	1.6949	0.6442	35.06	1.8352	0.6742	32.56	1.7094	0.6270
35.06	1.6861	0.6429	37.56	1.8589	0.6807	35.06	1.7001	0.6231
37.56	1.6785	0.6420	40.06	1.8783	0.6901	37.56	1.6913	0.6192
40.06	1.6719	0.6413	42.56	1.9219	0.7061	40.06	1.6829	0.6153
42.56	1.6661	0.6409	45.06	1.9703	0.7240	42.56	1.6744	0.6114
45.06	1.6611	0.6405	47.56	2.0449	0.7439	45.06	1.6661	0.6075
47.56	1.6568	0.6402	50.06	2.0899	0.7531	47.56	1.6581	0.6036
49.06	1.6531	0.6400	52.56	2.0803	0.7644	50.06	1.6504	0.6000
51.06	1.6499	0.6398				52.56	1.6431	0.5964
53.06	1.6471	0.6396				55.06	1.6364	0.5929
55.06	1.6447	0.6394				57.56	1.6304	0.5894
57.56	1.6425	0.6392				60.06	1.6250	0.5860
60.06	1.6404	0.6390				62.56	1.6203	0.5826
62.56	1.6385	0.6388				65.06	1.6161	0.5792
65.06	1.6367	0.6386				67.56	1.6124	0.5759
67.56	1.6350	0.6384				70.06	1.6091	0.5726
70.06	1.6334	0.6382				72.56	1.6061	0.5693
72.56	1.6319	0.6380				75.06	1.6034	0.5660
75.06	1.6304	0.6378				77.56	1.6010	0.5627
77.56	1.6290	0.6376				80.06	1.5987	0.5594
80.06	1.6276	0.6374				82.56	1.5966	0.5561
82.56	1.6263	0.6372				85.06	1.5946	0.5528
85.06	1.6250	0.6370				87.56	1.5927	0.5495
87.56	1.6238	0.6368				90.06	1.5909	0.5462
90.06	1.6226	0.6366				92.56	1.5892	0.5429
92.56	1.6214	0.6364				95.06	1.5876	0.5396
95.06	1.6203	0.6362				97.56	1.5861	0.5363
97.56	1.6192	0.6360				100.06	1.5847	0.5330
100.06	1.6181	0.6358						

Table AVI. Isothermal compressibility of
Ottawa banding sand specimen 29.
 $n = 0.373$ $S_1 = 25.2\%$

Pressure kbars	Volume cm ³	Relative Volume
0.00	2.7220	1.0000
0.50	2.5746	0.9453
1.25	2.4056	0.8833
2.51	2.2321	0.8200
3.76	2.1265	0.7812
5.01	2.0634	0.7530
6.27	2.0009	0.7424
7.52	1.9459	0.7296
8.78	1.9160	0.7112
10.03	1.8963	0.6969
11.28	1.8737	0.6802
12.53	1.8635	0.6740
13.78	1.8475	0.6637
15.03	1.8240	0.6467
16.28	1.8100	0.6313
17.53	1.7933	0.6160
18.78	1.7773	0.6005
20.03	1.7620	0.5849
21.28	1.7475	0.5693
22.53	1.7327	0.5531
23.78	1.7172	0.5369
25.03	1.7020	0.5205
26.28	1.6867	0.5040
27.53	1.6713	0.4875
28.78	1.6558	0.4712
30.03	1.6403	0.4548
31.28	1.6248	0.4384
32.53	1.6093	0.4220
33.78	1.5938	0.4056
35.03	1.5783	0.3892
36.28	1.5628	0.3728
37.53	1.5473	0.3564
38.78	1.5318	0.3400
40.03	1.5163	0.3236
41.28	1.5008	0.3072
42.53	1.4853	0.2908
43.78	1.4698	0.2744
45.03	1.4543	0.2580
46.28	1.4388	0.2416
47.53	1.4233	0.2252
48.78	1.4078	0.2088
50.03	1.3923	0.1924
51.28	1.3768	0.1760
52.53	1.3613	0.1596
53.78	1.3458	0.1432
55.03	1.3303	0.1268
56.28	1.3148	0.1104
57.53	1.2993	0.0940
58.78	1.2838	0.0776
60.03	1.2683	0.0612
61.28	1.2528	0.0448
62.53	1.2373	0.0284
63.78	1.2218	0.0120
65.03	1.2063	0.0000

Table AVII. Isothermal compressibility of
Ottawa banding sand specimen 33.
 $n = 0.372$ $S_1 = 25.1\%$

Pressure kbars	Volume cm ³	Relative Volume
0.00	2.7220	1.0000
0.25	2.6776	0.9837
0.50	2.5713	0.9446
1.25	2.3609	0.8673
2.51	2.1791	0.8006
3.76	2.0210	0.7425
5.01	1.9235	0.7136
6.27	1.8926	0.6933
7.52	1.8552	0.6816
8.78	1.8351	0.6742
10.03	1.8227	0.6696
11.28	1.8083	0.6633
12.53	1.7934	0.6511
13.78	1.7787	0.6449
15.03	1.7723	0.6313
16.28	1.7620	0.6247
17.53	1.7475	0.6167
18.78	1.7309	0.6030
20.03	1.7133	0.5893
21.28	1.6958	0.5757
22.53	1.6783	0.5620
23.78	1.6608	0.5484
25.03	1.6433	0.5347
26.28	1.6258	0.5210
27.53	1.6083	0.5073
28.78	1.5908	0.4936
30.03	1.5733	0.4799
31.28	1.5558	0.4662
32.53	1.5383	0.4525
33.78	1.5208	0.4388
35.03	1.5033	0.4251
36.28	1.4858	0.4114
37.53	1.4683	0.3977
38.78	1.4508	0.3840
40.03	1.4333	0.3703
41.28	1.4158	0.3566
42.53	1.3983	0.3429
43.78	1.3808	0.3292
45.03	1.3633	0.3155
46.28	1.3458	0.3018
47.53	1.3283	0.2881
48.78	1.3108	0.2744
50.03	1.2933	0.2607
51.28	1.2758	0.2470
52.53	1.2583	0.2333
53.78	1.2408	0.2196
55.03	1.2233	0.2059
56.28	1.2058	0.1922
57.53	1.1883	0.1785
58.78	1.1708	0.1648
60.03	1.1533	0.1511
61.28	1.1358	0.1374
62.53	1.1183	0.1237
63.78	1.1008	0.1100
65.03	1.0833	0.0963

Table AVIII. Isothermal compressibility of
Ottawa banding sand specimen 28.
 $n = 0.373$ $S_1 = 50.9\%$

Pressure kbars	Volume cm ³	Relative Volume
0.00	2.7220	1.0000
0.25	2.6563	0.9759
0.50	2.6099	0.9588
0.75	2.5668	0.9430
1.00	2.5296	0.9257
1.25	2.4319	0.9113
1.50	2.4050	0.8835
1.75	2.3325	0.8496
2.00	2.2877	0.8337
2.25	2.2319	0.8132
2.50	2.1801	0.7932
2.75	2.1001	0.7715
3.00	2.0351	0.7460
3.25	2.0095	0.7362
3.50	2.0164	0.7323
3.75	2.0101	0.7315
4.00	2.0030	0.7309
4.25	1.9939	0.7325
4.50	1.9905	0.7313
4.75	1.9822	0.7282
5.00	1.9756	0.7295
5.25	1.9773	0.7301
5.50	1.9698	0.7310
5.75	1.9628	0.7321
6.00	1.9550	0.7347
6.25	2.0079	0.7369
6.50	2.0153	0.7406
6.75	2.0349	0.7476
7.00	2.0475	0.7522
7.25	2.0845	0.7693
7.50	2.1445	0.7979
7.75	2.1986	0.8077
8.00	2.2164	0.8143

Table AXL Isothermal compressibility of
Ottawa banding sand specimen 1.

n = 0.378 S _i = 100%			
Pressure kbars	Volume cm ³	Relative Volume	
0.00	2.6070	1.0000	
1.00	2.5731	0.9889	
1.18	2.4637	0.9393	
2.51	2.4085	0.9239	
4.69	2.3668	0.9077	
4.79	2.3689	0.8956	
6.34	2.2687	0.8779	
6.64	2.2560	0.8694	
7.52	2.2476	0.8621	
10.03	2.2304	0.8555	
12.53	2.2156	0.8499	
15.04	2.2009	0.8450	
17.54	2.1900	0.8401	
20.05	2.1830	0.8377	
21.30	2.1805	0.8374	
23.81	2.1330	0.8101	
25.06	2.1205	0.8060	
26.32	2.1180	0.8123	
28.56	2.1011	0.8174	
31.30	2.1310	0.8235	
34.69	2.1716	0.8330	
38.00	2.1738	0.8377	
41.01	2.1900	0.8401	
44.50	2.2009	0.8450	
48.04	2.2196	0.8555	
51.03	2.2304	0.8621	
54.64	2.2476	0.8694	
58.34	2.2560	0.8779	
61.79	2.3059	0.8856	
65.68	2.3668	0.9077	
69.39	2.4085	0.9239	
73.57	2.4637	0.9393	
78.00	2.5731	0.9889	
82.70	2.6070	1.0000	

Table AX. Isothermal compressibility of
Ottawa banding sand specimen 34.

n = 0.373 S _i = 75.1%			
Pressure kbars	Volume cm ³	Relative Volume	
0.00	2.7220	1.0000	
1.25	2.5790	0.9475	
2.00	2.4432	0.8976	
2.51	2.3445	0.8760	
3.01	2.3416	0.8602	
3.76	2.3440	0.8501	
5.01	2.2900	0.8413	
6.77	2.2644	0.8319	
7.02	2.4175	0.8811	
10.03	2.2136	0.8132	
12.53	2.1153	0.7825	
15.04	2.1653	0.7955	
17.54	2.1511	0.7903	
20.05	2.1398	0.7861	
22.56	2.1293	0.7824	
25.06	2.1210	0.7792	
27.32	2.1114	0.7757	
30.00	2.0990	0.7711	
32.72	2.0820	0.7649	
35.06	2.0920	0.7635	
37.31	2.1073	0.7742	
40.00	2.1222	0.7796	
42.56	2.1210	0.7792	
45.05	2.1299	0.7834	
47.54	2.1377	0.7857	
50.03	2.1471	0.7888	
52.53	2.1563	0.7922	
55.03	2.1684	0.7966	
57.52	2.1831	0.8020	
60.00	2.1922	0.8054	
62.52	2.2096	0.8117	
65.01	2.2203	0.8157	
67.51	2.2317	0.8199	
70.00	2.2391	0.8240	
72.51	2.3131	0.8519	
75.00	2.3587	0.8651	
77.51	2.4457	0.8915	
80.00	2.4674	0.9065	

Table AIX. Isothermal compressibility of
Ottawa banding sand specimen 17.

n = 0.427 S _i = 55.7%			
Pressure kbars	Volume cm ³	Relative Volume	
0.00	2.7110	1.0000	
0.25	2.5776	0.9434	
0.50	2.4941	0.9200	
0.75	2.4400	0.9000	
1.00	2.3895	0.8810	
1.25	2.3480	0.8661	
1.50	2.3110	0.8525	
1.75	2.2723	0.8382	
2.00	2.2341	0.8241	
2.26	2.1949	0.8096	
2.51	2.1538	0.7945	
2.76	2.1297	0.7856	
3.01	2.1071	0.7772	
3.26	2.0986	0.7741	
3.51	2.0938	0.7716	
3.76	2.0868	0.7693	
4.01	2.0809	0.7671	
4.26	2.0752	0.7650	
4.51	2.0695	0.7629	
4.76	2.0638	0.7608	
5.01	2.0581	0.7587	
5.26	2.0524	0.7566	
5.51	2.0467	0.7545	
5.76	2.0410	0.7524	
6.01	2.0353	0.7503	
6.26	2.0296	0.7482	
6.51	2.0239	0.7461	
6.76	2.0182	0.7440	
7.01	2.0125	0.7419	
7.26	2.0068	0.7398	
7.51	1.9955	0.7361	
7.76	1.9783	0.7297	
8.01	1.9629	0.7240	
8.26	1.9523	0.7202	
8.51	1.9431	0.7167	
8.76	1.9368	0.7143	
9.01	1.9317	0.7099	
9.26	1.9247	0.7026	
9.51	1.9194	0.6932	
9.76	1.9139	0.7004	
10.01	1.9168	0.7071	
10.26	1.9206	0.7114	
10.51	1.9266	0.7143	
10.76	1.9348	0.7176	
11.01	1.9339	0.7207	
11.26	1.9369	0.7244	
11.51	1.9765	0.7291	
11.76	1.9306	0.7306	
12.01	2.0016	0.7383	
12.26	2.0184	0.7445	
12.51	2.0232	0.7470	
12.76	2.0535	0.7575	
13.01	2.0687	0.7681	
13.26	2.0912	0.7774	
13.51	2.1251	0.7939	
13.76	2.2036	0.8147	
14.01	2.2136	0.8147	

Table AXIII. Isothermal compressibility of Ottawa banding sand specimen 24.

$S_1 = 100\%$			
$n = 0.373$			
COMPRESSION No. 1			
Press.	Vol.	Rel.	
kbars	cm ³	Vol.	
0.00	2.7150	1.0000	
0.25	2.6979	0.9978	
1.00	2.6790	0.9957	
1.25	2.5375	0.9939	
1.50	2.5136	0.9925	
3.76	2.4370	0.9840	
5.01	2.3968	0.9805	
5.51	2.3375	0.9767	
6.77	2.3168	0.9720	
7.27	2.2767	0.9682	
10.03	2.2373	0.9618	
13.05	2.2092	0.9572	
20.05	2.2037	0.9501	
21.30	2.1972	0.9490	
22.56	2.1855	0.9456	
23.81	2.1802	0.9421	
27.57	2.1665	0.9390	
28.56	2.1606	0.9366	
29.32	2.1553	0.9346	
29.57	2.1506	0.9321	
29.56	2.1456	0.9299	
29.56	2.1406	0.9277	
29.56	2.1356	0.9255	
29.56	2.1306	0.9233	
29.56	2.1256	0.9211	
29.56	2.1206	0.9189	
29.56	2.1156	0.9167	
29.56	2.1106	0.9145	
29.56	2.1056	0.9123	
29.56	2.1006	0.9101	
29.56	2.0956	0.9079	
29.56	2.0906	0.9057	
29.56	2.0856	0.9035	
29.56	2.0806	0.9013	
29.56	2.0756	0.8991	
29.56	2.0706	0.8969	
29.56	2.0656	0.8947	
29.56	2.0606	0.8925	
29.56	2.0556	0.8903	
29.56	2.0506	0.8881	
29.56	2.0456	0.8859	
29.56	2.0406	0.8837	
29.56	2.0356	0.8815	
29.56	2.0306	0.8793	
29.56	2.0256	0.8771	
29.56	2.0206	0.8749	
29.56	2.0156	0.8727	
29.56	2.0106	0.8705	
29.56	2.0056	0.8683	
29.56	2.0006	0.8661	
29.56	1.9956	0.8639	
29.56	1.9906	0.8617	
29.56	1.9856	0.8595	
29.56	1.9806	0.8573	
29.56	1.9756	0.8551	
29.56	1.9706	0.8529	
29.56	1.9656	0.8507	
29.56	1.9606	0.8485	
29.56	1.9556	0.8463	
29.56	1.9506	0.8441	
29.56	1.9456	0.8419	
29.56	1.9406	0.8397	
29.56	1.9356	0.8375	
29.56	1.9306	0.8353	
29.56	1.9256	0.8331	
29.56	1.9206	0.8309	
29.56	1.9156	0.8287	
29.56	1.9106	0.8265	
29.56	1.9056	0.8243	
29.56	1.9006	0.8221	
29.56	1.8956	0.8199	
29.56	1.8906	0.8177	
29.56	1.8856	0.8155	
29.56	1.8806	0.8133	
29.56	1.8756	0.8111	
29.56	1.8706	0.8089	
29.56	1.8656	0.8067	
29.56	1.8606	0.8045	
29.56	1.8556	0.8023	
29.56	1.8506	0.8001	
29.56	1.8456	0.7979	
29.56	1.8406	0.7957	
29.56	1.8356	0.7935	
29.56	1.8306	0.7913	
29.56	1.8256	0.7891	
29.56	1.8206	0.7869	
29.56	1.8156	0.7847	
29.56	1.8106	0.7825	
29.56	1.8056	0.7803	
29.56	1.8006	0.7781	
29.56	1.7956	0.7759	
29.56	1.7906	0.7737	
29.56	1.7856	0.7715	
29.56	1.7806	0.7693	
29.56	1.7756	0.7671	
29.56	1.7706	0.7649	
29.56	1.7656	0.7627	
29.56	1.7606	0.7605	
29.56	1.7556	0.7583	
29.56	1.7506	0.7561	
29.56	1.7456	0.7539	
29.56	1.7406	0.7517	
29.56	1.7356	0.7495	
29.56	1.7306	0.7473	
29.56	1.7256	0.7451	
29.56	1.7206	0.7429	
29.56	1.7156	0.7407	
29.56	1.7106	0.7385	
29.56	1.7056	0.7363	
29.56	1.7006	0.7341	
29.56	1.6956	0.7319	
29.56	1.6906	0.7297	
29.56	1.6856	0.7275	
29.56	1.6806	0.7253	
29.56	1.6756	0.7231	
29.56	1.6706	0.7209	
29.56	1.6656	0.7187	
29.56	1.6606	0.7165	
29.56	1.6556	0.7143	
29.56	1.6506	0.7121	
29.56	1.6456	0.7099	
29.56	1.6406	0.7077	
29.56	1.6356	0.7055	
29.56	1.6306	0.7033	
29.56	1.6256	0.7011	
29.56	1.6206	0.6989	
29.56	1.6156	0.6967	
29.56	1.6106	0.6945	
29.56	1.6056	0.6923	
29.56	1.6006	0.6901	
29.56	1.5956	0.6879	
29.56	1.5906	0.6857	
29.56	1.5856	0.6835	
29.56	1.5806	0.6813	
29.56	1.5756	0.6791	
29.56	1.5706	0.6769	
29.56	1.5656	0.6747	
29.56	1.5606	0.6725	
29.56	1.5556	0.6703	
29.56	1.5506	0.6681	
29.56	1.5456	0.6659	
29.56	1.5406	0.6637	
29.56	1.5356	0.6615	
29.56	1.5306	0.6593	
29.56	1.5256	0.6571	
29.56	1.5206	0.6549	
29.56	1.5156	0.6527	
29.56	1.5106	0.6505	
29.56	1.5056	0.6483	
29.56	1.5006	0.6461	
29.56	1.4956	0.6439	
29.56	1.4906	0.6417	
29.56	1.4856	0.6395	
29.56	1.4806	0.6373	
29.56	1.4756	0.6351	
29.56	1.4706	0.6329	
29.56	1.4656	0.6307	
29.56	1.4606	0.6285	
29.56	1.4556	0.6263	
29.56	1.4506	0.6241	
29.56	1.4456	0.6219	
29.56	1.4406	0.6197	
29.56	1.4356	0.6175	
29.56	1.4306	0.6153	
29.56	1.4256	0.6131	
29.56	1.4206	0.6109	
29.56	1.4156	0.6087	
29.56	1.4106	0.6065	
29.56	1.4056	0.6043	
29.56	1.4006	0.6021	
29.56	1.3956	0.5999	
29.56	1.3906	0.5977	
29.56	1.3856	0.5955	
29.56	1.3806	0.5933	
29.56	1.3756	0.5911	
29.56	1.3706	0.5889	
29.56	1.3656	0.5867	
29.56	1.3606	0.5845	
29.56	1.3556	0.5823	
29.56	1.3506	0.5801	
29.56	1.3456	0.5779	
29.56	1.3406	0.5757	
29.56	1.3356	0.5735	
29.56	1.3306	0.5713	
29.56	1.3256	0.5691	
29.56	1.3206	0.5669	
29.56	1.3156	0.5647	
29.56	1.3106	0.5625	
29.56	1.3056	0.5603	
29.56	1.3006	0.5581	
29.56	1.2956	0.5559	
29.56	1.2906	0.5537	
29.56	1.2856	0.5515	
29.56	1.2806	0.5493	
29.56	1.2756	0.5471	
29.56	1.2706	0.5449	
29.56	1.2656	0.5427	
29.56	1.2606	0.5405	
29.56	1.2556	0.5383	
29.56	1.2506	0.5361	
29.56	1.2456	0.5339	
29.56	1.2406	0.5317	
29.56	1.2356	0.5295	
29.56	1.2306	0.5273	
29.56	1.2256	0.5251	
29.56	1.2206	0.5229	
29.56	1.2156	0.5207	
29.56	1.2106	0.5185	
29.56	1.2056	0.5163	
29.56	1.2006	0.5141	
29.56	1.1956	0.5119	
29.56	1.1906	0.5097	
29.56	1.1856	0.5075	
29.56	1.1806	0.5053	
29.56	1.1756	0.5031	
29.56	1.1706	0.5009	
29.56	1.1656	0.4987	
29.56	1.1606	0.4965	
29.56	1.1556	0.4943	
29.56	1.1506	0.4921	
29.56	1.1456	0.4899	
29.56	1.1406	0.4877	
29.56	1.1356	0.4855	
29.56	1.1306	0.4833	
29.56	1.1256	0.4811	
29.56	1.1206	0.4789	
29.56	1.1156	0.4767	
29.56	1.1106	0.4745	
29.56	1.1056	0.4723	
29.56	1.1006	0.4701	
29.56	1.0956	0.4679	
29.56	1.0906	0.4657	
29.56	1.0856	0.4635	
29.56	1.0806	0.4613	
29.56	1.0756	0.4591	
29.56	1.0706	0.4569	
29.56	1.0656	0.4547	
29.56	1.0606	0.4525	
29.56	1.0556	0.4503	
29.56	1.0506	0.4481	
29.56	1.0456	0.4459	
29.56	1.0406	0.4437	
29.56	1.0356	0.4415	
29.56	1.0306	0.4393	
29.56	1.0256	0.4371	
29.56	1.0206	0.4349	
29.56	1.0156	0.4327	
29.56	1.0106	0.4305	
29.56	1.0056	0.4283	
29.56	1.0006	0.4261	
29.56	0.9956	0.4239	
29.56	0.9906	0.4217	
29.56	0.9856	0.4195	
29.56	0.9806	0.4173	
29.56	0.9756	0.4151	
29.56	0.9706	0.4129	
29.56	0.9656	0.4107	
29.56	0.9606	0.4085	
29.56	0.9556	0.4063	
29.56	0.9506	0.4041	
29.56	0.9456	0.4019	
29.56	0.9406	0.3997	
29.56	0.9356	0.3975	
29.56	0.9306	0.3953	
29.56	0.9256	0.3931	
29.56	0.9206	0.3909	
29.56	0.9156	0.3887	
29.56	0.9106	0.3865	
29.56	0.9056	0.3843	
29.56	0.9006	0.3821	
29.56	0.8956	0.3799	
29.56	0.8906	0.3777	
29.56	0.8856	0.3755	
29.56	0.8806	0.3733	
29.56	0.8756	0.3711	
29.56	0.8706	0.3689	
29.56	0.8656	0.3667	
29.56	0.8606	0.3645	
29.56	0.8556	0.3623	
29.56	0.8506	0.3601	
29.56	0.8456	0.3579	
29.56	0.8406	0.3557	
29.56	0.8356	0.3535	
29.56	0.8306	0.3513	
29.56	0.8256	0.3491	
29.56	0.8206	0.3469	
29.5			

Table AXIV. Isothermal compressibility of
Ottawa banding sand specimen 27.

n = 0.373 $S_1 = 100\%$			
Pressure kbars	Volume cm ³	Relative Volume	
0.00	2.7220	1.0000	
0.50	2.7030	0.9930	
1.13	2.5665	0.9429	
2.51	2.5229	0.9268	
4.56	2.4751	0.9093	
5.01	2.4162	0.8977	
6.62	2.3886	0.8775	
7.02	2.3036	0.8757	
7.12	2.3630	0.8811	
7.12	2.3502	0.8694	
10.03	2.3352	0.8579	
12.53	2.3197	0.8522	
15.04	2.3059	0.8471	
17.54	2.2936	0.8426	
20.05	2.2817	0.8382	
21.30	2.2760	0.8361	
22.56	2.2661	0.8325	
23.11	2.2462	0.8252	
25.06	2.2309	0.8196	
27.57	2.2097	0.8114	
28.06	2.2241	0.8171	
28.51	2.2293	0.8190	
28.56	2.2401	0.8232	
31.30	2.2600	0.8301	
30.05	2.2733	0.8370	
31.30	2.2716	0.8404	
37.54	2.2936	0.8426	
38.59	2.3059	0.8471	
40.03	2.3197	0.8522	
40.03	2.3352	0.8579	
40.03	2.3502	0.8634	
40.03	2.3630	0.8681	
40.03	2.3617	0.8676	
40.03	2.3759	0.8740	
40.03	2.4162	0.8877	
40.03	2.4751	0.9093	
40.03	2.5229	0.9268	
40.03	2.5665	0.9429	
40.03	2.7030	0.9930	
40.03	2.7220	1.0000	

Table AXV. Isothermal compressibility of
West Lebanon glacial till specimen 40.

n = 0.354 $S_1 = 57.3\%$			
Pressure kbars	Volume cm ³	Relative Volume	
0.00	2.7390	1.0000	
0.12	2.5510	0.9314	
0.38	2.4704	0.9019	
0.63	2.4214	0.8841	
1.25	2.3503	0.8553	
1.63	2.3123	0.8444	
1.88	2.2374	0.8351	
2.91	2.2596	0.8250	
3.76	2.2324	0.8152	
6.00	2.2049	0.8050	
9.09	2.1930	0.8007	
7.52	2.1720	0.7930	
9.27	2.1707	0.7925	
11.77	2.1493	0.7847	
10.03	2.1406	0.7815	
12.53	2.1324	0.7735	
15.04	2.1251	0.7727	
17.54	2.1165	0.7727	
20.05	2.1104	0.7705	
22.56	2.1035	0.7650	
25.06	2.0967	0.7620	
26.12	2.0930	0.7622	
26.54	2.0860	0.7613	
28.07	2.0730	0.7569	
28.56	2.0446	0.7611	
30.05	2.0933	0.7642	
30.54	2.1006	0.7659	
35.04	2.1054	0.7657	
42.53	2.1341	0.7721	
40.03	2.1222	0.7743	
40.03	2.1328	0.7717	
40.03	2.1546	0.7856	
40.03	2.1707	0.7920	
40.03	2.2006	0.8034	
40.03	2.2308	0.8145	
40.03	2.2555	0.8230	
40.03	2.3267	0.8490	
40.03	2.3415	0.8549	

Table AXVI. Isothermal compressibility of
West Lebanon glacial till specimen 16.

n = 0.357 $S_1 = 58.3\%$			
Pressure kbars	Volume cm ³	Relative Volume	
0.00	2.7330	1.0000	
0.50	2.4356	0.8912	
1.00	2.3037	0.8429	
1.50	2.2643	0.8235	
2.51	2.2340	0.8174	
5.01	2.2062	0.8072	
6.77	2.1902	0.8014	
7.12	2.1759	0.7947	
9.22	2.1560	0.7839	
9.22	2.1422	0.7738	
11.22	2.1239	0.7790	
20.05	2.1036	0.7697	
22.56	2.0959	0.7669	
25.06	2.0919	0.7654	
27.57	2.0731	0.7606	
28.06	2.0793	0.7610	
28.56	2.0844	0.7627	
30.05	2.0954	0.7667	
32.73	2.1101	0.7721	
35.77	2.1403	0.7833	
40.03	2.1533	0.7934	
40.03	2.1337	0.7990	
40.03	2.1974	0.8400	
40.03	2.2532	0.8844	
40.03	2.3043	0.9311	
40.03	2.3165	0.9476	

Table AXVIII. Isothermal compressibility of West Lebanon glacial till specimen 42.

n = 0.358 $S_1 = 100\%$			
Pressure kbars	Volume cm ³	Relative Volume	Relative Volume
0.00	2.7230	1.0000	1.0000
0.83	2.7032	0.9927	0.9927
1.33	2.5825	0.9488	0.9488
1.75	2.5599	0.9401	0.9401
2.51	2.5363	0.9316	0.9316
4.01	2.5013	0.9186	0.9186
4.89	2.4507	0.9110	0.9110
5.01	2.4337	0.8945	0.8945
6.42	2.4154	0.8870	0.8870
6.77	2.3826	0.8750	0.8750
7.52	2.3754	0.8724	0.8724
10.03	2.3593	0.8668	0.8668
12.53	2.3443	0.8611	0.8611
15.04	2.3314	0.8562	0.8562
17.54	2.3191	0.8517	0.8517
20.05	2.3094	0.8431	0.8431
21.30	2.3039	0.8461	0.8461
22.56	2.2906	0.8412	0.8412
23.01	2.2601	0.8300	0.8300
23.06	2.2471	0.8252	0.8252
27.70	2.2343	0.8205	0.8205
25.06	2.2437	0.8240	0.8240
22.56	2.2503	0.8264	0.8264
21.30	2.2671	0.8326	0.8326
20.05	2.3000	0.8446	0.8446
18.30	2.3149	0.8501	0.8501
17.54	2.3191	0.8517	0.8517
15.04	2.3314	0.8562	0.8562
12.53	2.3443	0.8611	0.8611
10.03	2.3593	0.8668	0.8668
7.52	2.3754	0.8724	0.8724
6.77	2.3826	0.8750	0.8750
6.42	2.4154	0.8870	0.8870
5.01	2.4337	0.8945	0.8945
4.01	2.4751	0.9034	0.9034
4.89	2.5013	0.9110	0.9110
2.51	2.5363	0.9316	0.9316
1.75	2.5599	0.9401	0.9401
1.33	2.5825	0.9488	0.9488
0.83	2.7032	0.9927	0.9927
0.00	2.7230	1.0000	1.0000

Table AXVII. Isothermal compressibility of West Lebanon glacial till specimen 32.

n = 0.354 $S_1 = 100\%$			
Pressure kbars	Volume cm ³	Relative Volume	Relative Volume
0.00	2.7540	1.0000	1.0000
0.65	2.7398	0.9943	0.9943
1.23	2.6166	0.9501	0.9501
1.50	2.6009	0.9444	0.9444
2.51	2.5710	0.9335	0.9335
3.75	2.5433	0.9237	0.9237
4.94	2.5247	0.9167	0.9167
5.26	2.4795	0.9003	0.9003
5.76	2.4666	0.8956	0.8956
6.57	2.4571	0.8922	0.8922
7.02	2.4304	0.8825	0.8825
7.52	2.4263	0.8810	0.8810
10.03	2.4115	0.8756	0.8756
12.53	2.3915	0.8709	0.8709
15.04	2.3666	0.8666	0.8666
17.54	2.3750	0.8684	0.8684
20.05	2.3657	0.8690	0.8690
22.56	2.3552	0.8652	0.8652
23.31	2.3455	0.8617	0.8617
24.31	2.3321	0.8663	0.8663
25.06	2.3157	0.8603	0.8603
26.32	2.3057	0.8572	0.8572
28.32	2.2934	0.8546	0.8546
22.56	2.3257	0.8445	0.8445
21.30	2.3263	0.8449	0.8449
20.05	2.3557	0.8554	0.8554
19.30	2.3677	0.8597	0.8597
17.54	2.3750	0.8664	0.8664
15.04	2.3666	0.8666	0.8666
12.53	2.3995	0.8709	0.8709
10.03	2.4115	0.8756	0.8756
7.52	2.4263	0.8810	0.8810
7.02	2.4304	0.8825	0.8825
6.27	2.4369	0.8843	0.8843
6.02	2.4561	0.8915	0.8915
5.76	2.4666	0.8956	0.8956
4.76	2.4827	0.9015	0.9015
4.51	2.5030	0.9099	0.9099
1.26	2.5231	0.9161	0.9161
3.76	2.5430	0.9234	0.9234
2.51	2.5710	0.9335	0.9335
1.50	2.6009	0.9444	0.9444
1.25	2.6166	0.9501	0.9501
0.65	2.7398	0.9943	0.9943
0.00	2.7540	1.0000	1.0000

~~Security Classification~~

DOCUMENT CONTROL DATA - R & D

(Security classification of title, body of abstract and indexing annotation must be entered when the original report is classified)

1. ORIGINATING ACTIVITY (Corporate author) U.S. Army Cold Regions Research and Engineering Laboratory Hanover, N.H. 03755		2a. REPORT SECURITY CLASSIFICATION Unclassified	
		2b. GROUP	
3. REPORT TITLE THE ISOTHERMAL COMPRESSIBILITY OF FROZEN SOIL AND ICE TO 30 KILOBARS AT -10°C			
4. DESCRIPTIVE NOTES (Type of report and inclusive dates)			
5. AUTHOR(S) (First name, middle initial, last name) Edwin Chamberlain and Pieter Hoekstra			
6. REPORT DATE June 1970		7a. TOTAL NO. OF PAGES 38	7b. NO. OF REFS 19
8a. CONTRACT OR GRANT NO.		8b. ORIGINATOR'S REPORT NUMBER(S) Technical Report 225	
9. PROJECT NO. ARPA Order 968		9c. OTHER REPORT NO(S) (Any other numbers that may be assigned this report)	
10. DISTRIBUTION STATEMENT This document has been approved for public release and sale; its distribution is unlimited			
11. SUPPLEMENTARY NOTES		12. SPONSORING MILITARY ACTIVITY Advanced Research Projects Agency Washington, D.C. 20301	
13. ABSTRACT The isothermal compressibilities of ice and partially and fully saturated sand and silt at -10°C are presented. The tests employ a piston-die device with which a uniaxial load is imposed on a lead encapsulated specimen, resulting in the hydrostatic compression of the test specimen. Pressures to 30 kbars are obtained. The compressibility of ice is as reported by P.W. Bridgman. The various phase transformations of ice I to water to ice V to ice VI to ice VIII appear as expected. It is shown that the compressibility of frozen soil can be readily predicted from the knowledge of material properties such as degree of saturation with ice, porosity, and the compressibilities of the ice and mineral components.			
14. KEYWORDS Isothermal compressibility of frozen soils Isothermal compressibility of ice			